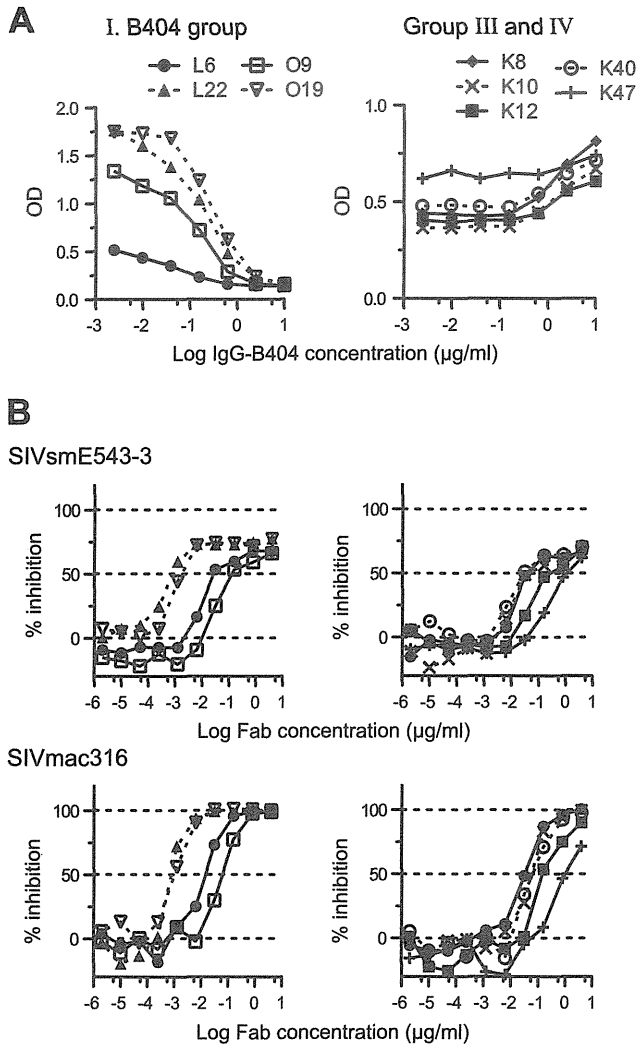

FIG 4 The specificity and potency of Fab clones in the B404 group are similar to those of B404. (A) Competition ELISA was performed using serially diluted B404 IgG as a competitor. B404 IgG significantly inhibited the binding of the Fabs in the B404 group (L6, L22, O9, and O19). In contrast, B404 IgG did not compete with the Fabs in groups III (K8 and K10) and IV (K12, K40, and K47) and even enhanced the binding of these Fabs. (B) Neutralization potencies of Fabs in the B404 group (left) and groups III and IV (right) are shown by inhibition of infection to TZM-bl cells with neutralization-resistant SIVsmE543-3 and genetically divergent SIVmac316.

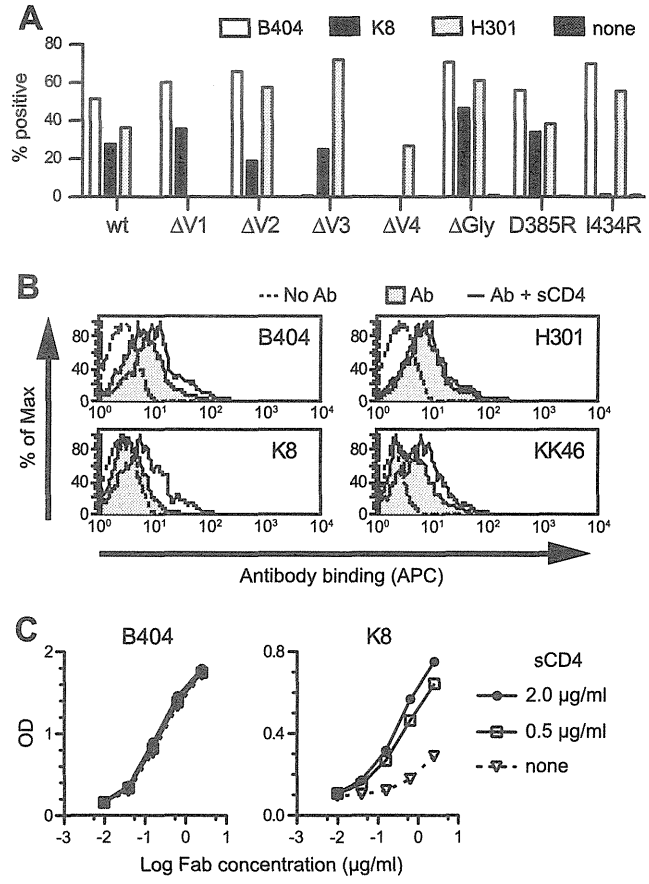

FIG 5 B404 recognizes a conformational epitope, including the V3 and V4 loops, and sCD4 enhances the exposure of the epitope in trimeric Env. (A) Reactivity of B404, K8, and H301 (anti-V1 Fab) to Env mutants was examined using 293T cells transfected with plasmids to express SIVsmE543-3 Env (wild-type), mutants with deletions in the V1 (ΔV1), V2 (ΔV2), V3 (ΔV3), and V4 (ΔV4) loops, an N306A/N316A/N349A mutant lacking glycosylation sites near the V3 loop (ΔGly), a D385R mutant interfering with CD4bs antibodies (D385R), and an I434R mutant interfering with CD4i antibodies (I434R). The transfected cells were stained with Fabs B404, K8, and H301, and the reactivity of Env mutants was analyzed using flow cytometry. The percentage of Fab^+ cells is shown. (B) Reactivity of Fabs B404, K8, and H301, and murine anti-V3 MAb KK46 to sCD4-treated trimeric Env on the cell surface. Cells transfected with the plasmid to express SIVsmE543-3 Env were incubated with 2 μg/ml sCD4 for 15 min, and the reactivities of antibodies were similarly examined. The tinted histogram represents cells stained by antibody in the absence of sCD4. The dotted line shows the unstained control. (C) Reactivity of Fab clones B404 and K8 to sCD4-treated monomeric Env. The reactivity of serially diluted Fab to Env was examined by ELISA using SIVsmE543-3 as an antigen in the absence or presence of 0.5 or 2.0 μg/ml sCD4.

tant lacking 3 glycosylation sites flanking the V3 loop (ΔGly) were constructed. In addition, mutants carrying single mutations in the CD4bs (D385R) and CD4i (I434R) sites, corresponding to D368R and I420R in HIV-1 gp120 (13, 44–46), were examined to clarify the relationship of the B404 epitope to the CD4bs and CD4i sites. Flow cytometry analysis using cells expressing these Env mutants revealed that the reactivity of B404 was completely lost in ΔV3 and ΔV4 mutants, though B404 bound to other mutants even better than it did to the wild type (Fig. 5A). These results suggested that B404 recognizes a conformational epitope consisting of the V3 and V4 loops.

The reactivity of another Fab, K8, which targets an epitope other than that of B404 (Fig. 4A), was lost in ΔV4 and I434R mutants (Fig. 5A). No reactivity to I434R strongly suggested that K8 is a CD4i antibody. Therefore, the effect of sCD4 ligation on antibody binding to Env trimers and monomers was examined using flow cytometry and ELISA, respectively. The reactivity of B404, K8, and KK46 (murine anti-V3 MAb) to Env on the cell surface was enhanced by the addition of sCD4, although no effect was observed in anti-V1 Fab H301 (Fig. 5B). This suggested that epitopes for B404, K8, and KK46 are exposed in the open conformation of the Env trimer triggered by CD4 binding. Consistent with the analysis of mutant Envs, the reactivity of K8 to Env monomer was enhanced by the addition of sCD4, but B404 showed no enhancement of reactivity (Fig. 5C).

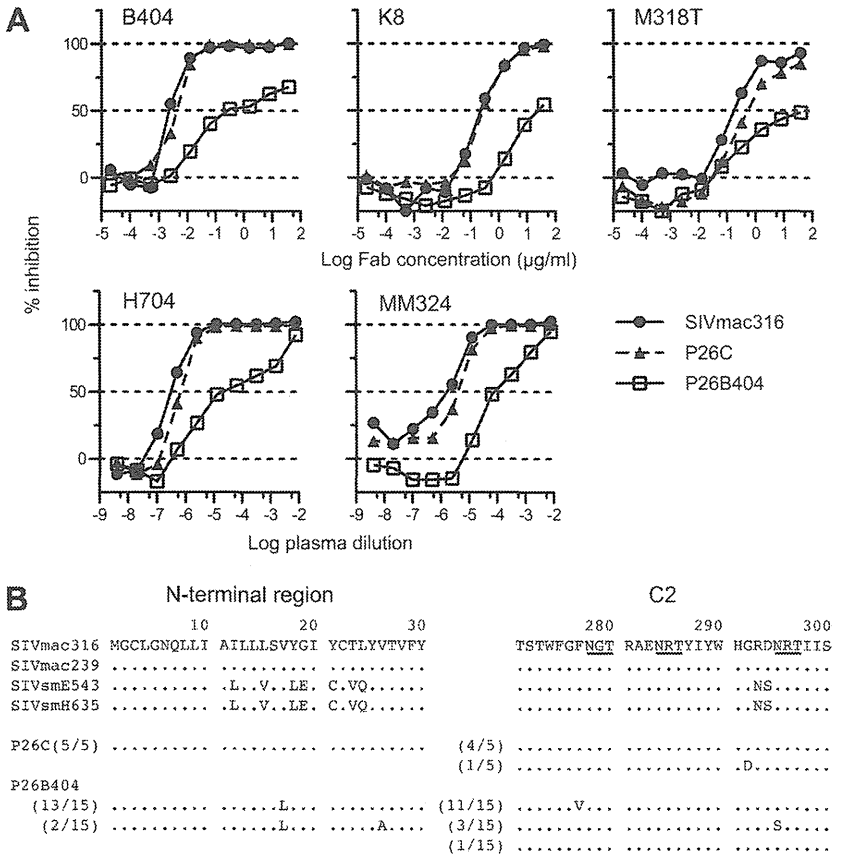

FIG 6 Isolation of variants resistant to B404 and amino acid substitutions in gp120. The B404-resistant variant was induced from SIVmac316 by passages of viruses in PM-1/CCR5 cells with increasing concentrations of B404 Fab. A B404-resistant variant, P26B404, was obtained from the supernatant of passage 26. P26C was obtained after 26 passages without B404. (A) The sensitivities of P26B404, P26C, and parental SIVmac316 to neutralization are shown by inhibition of infection of TZM-bl cells. B404 and K8 Fabs, murine MAb M318T, which recognizes the V2 of gp120, and plasma samples from SIVsmH635FC-infected macaque H704 and SIVmac239-infected macaque MM324 were used for the neutralization assay. (B) Amino acid sequences of the N-terminal and C2 regions of gp120 from P26C and P26B404 are aligned with those of parental SIVmac316 and SIV strains, SIVmac239, SIVsmE543-3 and SIVsmH635FC. The number of clones per total number of clones is given in parentheses. Identical amino acids are shown as dots, and potential glycosylation sites in SIVmac316 are indicated with underlining.

The enhancement by sCD4 of reactivity to both monomeric and trimeric Env and the interference in binding by the I434R (I420R in HIV-1) mutation in Env, which are features of so-called CD4i antibodies against HIV-1 (13, 45, 46), indicate that K8 targets the CD4i epitope. The enhanced reactivity of B404 by sCD4 to trimeric but not monomeric Env is analogous to the reactivity of anti-V3 antibodies (65). These results suggest that B404 recognizes a conformational epitope consisting of the V3 and V4 loops, which are intensely exposed on the Env trimer after CD4 ligation.

Selection of variants resistant to NAb B404. To select B404-resistant variants *in vitro*, we passaged SIVmac316, which is the most sensitive to B404 of the SIV strains tested (Fig. 1), in PM1/CCR5 cells in the presence of increasing concentrations of B404. As a control, passage under the same conditions without B404 was also performed to monitor spontaneous changes during infection in PM1/CCR5 cells. The concentration of B404 was increased from 5 ng/ml to 400 μg/ml at passage 26. Viruses recovered at passage 26 in the presence and absence of B404, which were designated P26B404 and P26C, respectively, were examined for their sensitivity to antibodies and plasma samples from SIV-infected macaques (Fig. 6A). The IC_{50} for B404 against SIVmac316, P26C, and P26B404 were 2.8, 4.1, and 240 ng/ml, respectively, showing an 86-fold resistance of P26B404 to B404 compared with that of wild-type SIVmac316. P26B404 was also resistant to neutralization by MAbs K8 (CD4i) and M318T (V2), which target epitopes other than that of B404, and plasma samples from SIV-infected macaques (Fig. 6A). These results suggested that P26B404 acquired resistance to antibody-mediated neutralization comparable to that observed in neutralization-resistant SIV strains, such as SIVmac239 and SIVsmE543-3. Sequence analysis of gp120 revealed 3 amino acid substitutions specific to P26B404: V17L in the N-terminal region and F277V and N295S in the C2 region (Fig. 6B). Of these substitutions, the two in the C2 region were highly conserved among SIVsm/mac and HIV-2 strains. These substitutions were independently observed, and no variant with both F277V and N295S was found in the 15 clones sequenced.

MD simulation of gp120 outer domains from B404-sensitive and B404-resistant variants. To address structural impacts of the 2 mutations in the C2 region, we performed MD simulation of unliganded gp120 outer domains from B404-sensitive (SIVmac316) and B404-resistant (F277V and N295S) variants. To map the sites at which structural dynamics were influenced by C2 mutations, we calculated the RMSF of the main chains of individual amino acid residues using 90,000 snapshots from 5 to 50 ns of

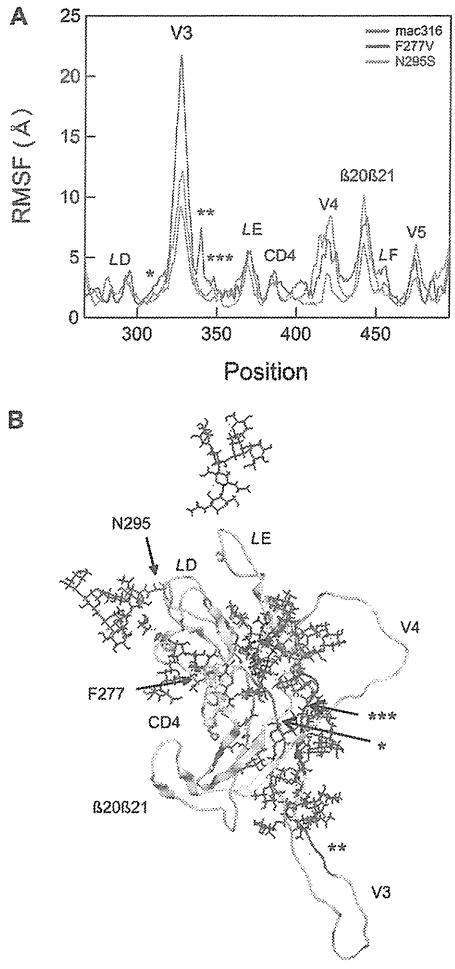

FIG 7 Effects of F277V and N295S mutations on the structural dynamics of the gp120 outer domain. (A) Distribution of RMSF in the gp120 outer domain. MD simulations of gp120 outer domains of SIVmac316, F277V, and N295S were carried out at 1 atm and 310 K for 50 ns as described in Materials and Methods. The RMSF values, which indicate the atomic fluctuations of the main chains of individual amino acids during MD simulations, were calculated using 90,000 snapshots from 9 to 50 ns of each MD simulation. The numbers on the horizontal axes indicate amino acid positions in gp120. The RMSF values of the mutants are significantly different from those of parental SIVmac316 at the V3 loop, the V3 flanking regions (indicated by asterisks), the V4 loop, the β20β21/*LF* loop, and the V5 loop regions. (B) A structure at 50 ns of MD simulation of the SIVmac316 gp120 outer domain is shown as a representative to indicate the steric location of mutation sites and various loops. The regions that are proximal to the V3/V4 loops and displayed fluctuations that differed from those of parental SIVmac316 (Fig. 7A) are highlighted in orange (*), blue (**), and purple (***). Green sticks indicate glycans.

each MD simulation (Fig. 7A). RMSF values provide key information about the atomic fluctuations of the individual amino acids of a protein in solution (57). These values were maximal at the tip of the V3 loop and prominent at other loop regions, including *LD*, *LE*, CD4 binding, V4, β20β21/*LF*, and V5 (Fig. 7A), suggesting that these loops fluctuate in solution. Notably, the F277V and N295S mutations were found to induce changes in RMSF values mainly at the V3, V4, β20β21/*LF*, and V5 loop regions (Fig. 7A, blue and green lines, respectively). Interestingly, these regions are located far from the C2 mutation sites compared with the locations of other loops, such as *LD*, *LE*, and CD4 binding, which had RMSF values that were similar among wild-type and B404-resistant variants (Fig. 7B; F277V in *LD* and N295S in the proximal region of *LD*). In particular, RMSF changes by the C2 mutations were the most prominent at the V3/V4 loops and their neighboring regions (Fig. 7). These results suggested that the F277V and N295S mutations could alter the structural dynamics of V3/V4 loops and their neighboring regions in solution. The structural alterations would lead to changes in entropy of the regions, which affect the binding affinity to B404. The finding is consistent with the results of an epitope mapping study of B404.

DISCUSSION

Potent and broadly neutralizing MAbs have recently been isolated from HIV-1-infected patients and analyzed to understand the mechanism of neutralization against a broad spectrum of HIV-1 strains and to design vaccines against their neutralizing epitopes (12–16). Although the SIV-macaque model has been used as an animal model for HIV-1 infection for vaccine development (6, 8, 24), no potent and broadly neutralizing monoclonal antibody against SIV was available. Therefore, the epitopes and mechanism for broad neutralization of SIV remained uncertain. Many monoclonal antibodies against SIVsm/mac were isolated from SIV-infected macaques (66, 67) and mice immunized with SIV Env (43, 47, 68), but few of them showed neutralizing activity against various SIV strains, including highly neutralization-resistant SIVmac239 (68). In comparison with these monoclonal antibodies against SIV identified so far, B404 apparently has a broadly neutralizing activity, which enables it to neutralize multiple, diverse SIV isolates, and can be defined as the first generation of broadly NAbs against SIV. The broad and potent neutralizing activity of B404 shown in this study indicates that B404 can be used to analyze broad neutralization against SIV. The B404 epitope, the newly identified broadly neutralizing epitope against SIV, will further understanding of the mechanism of broad neutralization effective for protection from SIV infection.

The infection of rhesus macaques with SIVsmH635FC, a highly neutralization-sensitive clone, was chosen for this study because this SIV strain induced a vigorous and potent antibody response in all the infected macaques and acquired many viral mutations to escape antibody recognition (25, 26). The kinetics of B404 neutralization against various SIV strains were similar to those observed in the plasma sample of the macaque from which B404 was isolated, suggesting that B404-like NAbs are representative of the neutralizing activity in SIVsmH635-infected macaque H723 (25). Consistent with this observation, B404-like NAbs were shown to be a major group in NAbs genetically and functionally. Most of the NAbs in the 4 SIVsmH635FC-infected macaques analyzed had the same features, including the use of a specific VH3 germ line and λ light chains, a long CDRH3 loop, and competition with B404. The bias in the specificity and gene usage may be partially enhanced by the screening process, because B404-like NAbs were predominantly isolated from λ light-chain libraries by panning against H301-conjugated Env. In addition, isolating antibodies against quaternary epitopes constituted by the Env trimer through panning using monomeric Env was difficult. However, the presence of many independent B404-like NAbs strongly suggests that B404-like NAbs compose a significant fraction of NAbs in 4 SIVsmH635FC-infected macaques. Moreover, the vigorous induction of B404-like NAbs in SIVsmH635FC-infected macaques was also supported by the multiple B cell origins apparent

from several subgroups in B404-like NAbs (Fig. 1). These subgroups originated from distinct B cell precursors generated by VDJ recombination, because they were often distinguished by the length and nucleotide sequences of CDRH3.

The observation of few B404-like NAbs from macaques infected with the SIV mix clearly indicates that induction of B404-like NAbs depends on infection with SIVsmH635FC. The exclusive induction of B404-like NAbs only in SIVsmH635FC-infected macaques also raises the possibility that Env from SIVsmH635FC is a highly immunogenic protein that induces antibodies against the B404 epitope. The use of Env from SIVsmH635FC for vaccination may be advantageous for the induction of broadly neutralizing antibodies, because the Env from an HIV-1-infected patient with broadly neutralizing antibodies induced cross-reactive anti-HIV-1 NAbs in an animal model (69). The Env in this vaccination study is capable of mediating CD4-independent infection. Since the Env of SIVsmH635FC has a mutation in the CD4-binding region (D385N), NAb induction may be affected by CD4 independency of Env. The development of vaccines aimed at inducing B404-like NAbs in rhesus macaques will be useful in establishing models for development of antibody-based vaccines targeting specific epitopes for broad neutralization.

Biased usage of a specific VH3 germ line gene and λ light chain are remarkable genetic features of B404-like NAbs. The induction of NAbs with specific germ line genes, such as VH1-69 for CD4i (70) and VH5-51 for V3 (64), is frequently observed in HIV-1-infected patients. A close relationship between VH germ line genes and target epitopes suggests the importance of Ig gene usage in the induction of broadly neutralizing antibodies. Therefore, rational design of vaccines has been undertaken based on reactivity to antibodies with the germ line genes used by known broadly neutralizing antibodies (11, 71, 72). Unfortunately, the VH3 germ line gene of B404 is divergent from all human VH3 germ line genes, suggesting the absence of a human counterpart. This may partially explain why B404-like NAbs have not been identified in HIV-infected humans, although the structure of HIV-1 Env, which is different from that of SIV, significantly affects immunogenicity of the B404 epitope. Rhesus macaque-specific germ line genes were also used by NAbs against the quaternary epitope of HIV-1 Env from simian and human immunodeficiency virus (SHIV)-infected macaques, but their germ line genes were different from the VH3 germ line gene used by B404 (73). Even in the presence of a human VH gene counterpart, the antibody response to a neutralizing epitope may differ between rhesus macaques and humans (74). In addition to the genetic diversity of germ line genes, the rhesus macaque CDRH3 repertoire differs from that of humans, resulting in species-specific antibody repertoires (75). This species specificity in antibody induction is a problem in the evaluation of HIV-1 vaccines in animal models, especially those designed for specific neutralizing epitopes of HIV-1. Conversely, K8, the CD4i NAb from a SIV-infected macaque, used the rhesus VH1 germ line gene, an analog of human VH1-69 frequently used by CD4i NAbs in HIV-1-infected humans (70). Thus, the mechanism of induction of CD4i NAbs with VH1-69 may be common in both humans and rhesus macaques. To analyze vaccine candidates properly in nonhuman primates, similarities and differences in antibody response between rhesus macaques and humans should be considered.

B404 recognizes a conformational epitope consisting of the V3 and V4 loops. The enhanced exposure of the epitope in trimeric Env by sCD4 and efficient neutralization of neutralization-resistant SIV strains by the scFv form of B404 suggests that the B404 epitope is sterically masked by the V1/V2 loops and glycans, analogous to CD4i and V3 epitopes (46, 65, 76). Consistent with this interpretation, B404 reacted more intensely to Env mutants lacking the V1 and V2 loops than to the wild-type Env. MD simulation supported these observations by indicating changes in the structural dynamics of V3/V4 loops and their neighboring regions in gp120 of resistant variants with F277V and N295S mutations in the C2 region. The acquisition of resistance to the broadly neutralizing antibodies b12, PG9, and PG16 due to C2 mutations far from the target epitopes was also observed in HIV-1 CRF01_AE (77, 78). MD simulation is a powerful computational method for analyzing structural dynamics of proteins in solution on the basis of theoretical and empirical principles in physical chemistry (79) and has been applied to research on viruses (80). The structural dynamics of protein surfaces in solution plays a key role in protein interactions, and MD simulation is advantageous in speculation about interactions between proteins containing flexible regions, such as V3 and V4 loops. Analysis of fluctuation changes in mutant proteins is useful to identify the regions which affect protein-protein interaction.

Although the V3 and V4 loops are known to contain linear epitopes for antibody-mediated neutralization in SIV infection, no conformational MAb against SIV with characteristics similar to those of B404 has been reported (43, 47, 66–68). Several MAbs to conformational epitopes that include the V3 region, such as PGT antibodies, represented by PGT128 (15, 19), 3BC176, and 3BC315 (81), were isolated from HIV-1-infected patients. The PGT128 epitope consists of the short segment of the V3 loop and 2 neighboring glycans (19), but the binding of B404 is independent of these glycans near the V3 region. The epitope of 3BC176 and 3BC315 is close to the V3 loop, and their binding is partially enhanced by CD4 binding, similar to that of B404 (81). However, in contrast to B404, 3BC176 and 3BC315 do not bind to monomeric Env and compete with CD4i antibodies, suggesting that their epitope is different from that of B404. Although we have not determined the precise B404 epitope, the characteristics of B404 that are similar to those of CD4i and V3 antibodies suggest that B404 recognizes a conserved region important for binding to the CCR5 coreceptor (46, 65, 76, 82).

Despite recent progress in understanding the broad neutralization of HIV-1, epitopes for potent and broad neutralization have not been analyzed in an SIV model because NAb analysis using SIV cannot be directly applied to HIV-1. The main disadvantage of SIV is the antigenicity difference relative to HIV-1, which makes examination of neutralizing epitopes of HIV-1 impossible. Although the use of SHIV expressing HIV-1 Env enables the evaluation of vaccine candidates designed for target epitopes of HIV-1 in nonhuman primates, an SIV model was more predictive of vaccine efficacy than a SHIV model in clinical trials of a T-cell-based vaccine (83, 84). For comprehensive assessment of immunity induced by vaccine candidates, proof-of-concept trials using the SIV model should be considered before further efficacy trials. The identification of B404 with its potent and broad neutralizing activity against SIV will be a useful adjunct for evaluating the mechanism of neutralization in an SIV-macaque model and will contribute to the development of HIV-1 vaccines.

ACKNOWLEDGMENTS

We thank Yuko Katsumata for excellent assistance. The phagemid vector pComb3X was kindly provided by the Scripps Research Institute. The following reagents were obtained through the NIH AIDS Research and Reference Reagent Program, Division of AIDS, NIAID, NIH: TZM-bl cells from John C. Kappes, Xiaoyun Wu, and Tranzyme Inc. and KK46 from Karen Kent and Caroline Powell.

This work was supported in part by the Special Coordination Funds for Promoting Science and Technology, the Program of Founding Research Centres for Emerging and Re-emerging Infectious Diseases, the Global COE program Global Education and Research Centre Aiming at the Control of AIDS, a grant-in-aid for scientific research (C-24591484) from the Ministry of Education, Culture, Sport, Science and Technology, Japan, and a grant from the Ministry of Health, Welfare and Labor of Japan (H24-AIDS-007).

REFERENCES

1. **Igarashi T, Brown C, Azadegan A, Haigwood N, Dimitrov D, Martin MA, Shibata R.** 1999. Human immunodeficiency virus type 1 neutralizing antibodies accelerate clearance of cell-free virions from blood plasma. Nat. Med. 5:211–216.
2. **Shibata R, Igarashi T, Haigwood N, Buckler-White A, Ogert R, Ross W, Willey R, Cho MW, Martin MA.** 1999. Neutralizing antibody directed against the HIV-1 envelope glycoprotein can completely block HIV-1/SIV chimeric virus infections of macaque monkeys. Nat. Med. 5:204–210.
3. **Veazey RS, Shattock RJ, Pope M, Kirijan JC, Jones J, Hu Q, Ketas T, Marx PA, Klasse PJ, Burton DR, Moore JP.** 2003. Prevention of virus transmission to macaque monkeys by a vaginally applied monoclonal antibody to HIV-1 gp120. Nat. Med. 9:343–346.
4. **Hessell AJ, Rakasz EG, Poignard P, Hangartner L, Landucci G, Forthal DN, Koff WC, Watkins DI, Burton DR.** 2009. Broadly neutralizing human anti-HIV antibody 2G12 is effective in protection against mucosal SHIV challenge even at low serum neutralizing titers. PLoS Pathog. 5:e1000433. doi:10.1371/journal.ppat.1000433.
5. **Mascola JR, Stiegler G, VanCott TC, Katinger H, Carpenter CB, Hanson CE, Beary H, Hayes D, Frankel SS, Birx DL, Lewis MG.** 2000. Protection of macaques against vaginal transmission of a pathogenic HIV-1/SIV chimeric virus by passive infusion of neutralizing antibodies. Nat. Med. 6:207–210.
6. **Ourmanov I, Kuwata T, Goeken R, Goldstein S, Iyengar R, Buckler-White A, Lafont B, Hirsch VM.** 2009. Improved survival in rhesus macaques immunized with modified vaccinia virus Ankara recombinants expressing simian immunodeficiency virus envelope correlates with reduction in memory CD4+ T-cell loss and higher titers of neutralizing antibody. J. Virol. 83:5388–5400.
7. **Bogers WM, Davis D, Baak I, Kan E, Hofman S, Sun Y, Mortier D, Lian Y, Oostermeijer H, Fagrouch Z, Dubbes R, van der Maas M, Mooij P, Koopman G, Verschoor E, Langedijk JP, Zhao J, Brocca-Cofano E, Robert-Guroff M, Srivastava I, Barnett S, Heeney JL.** 2008. Systemic neutralizing antibodies induced by long interval mucosally primed systemically boosted immunization correlate with protection from mucosal SHIV challenge. Virology 382:217–225.
8. **Flatz L, Cheng C, Wang L, Foulds KE, Ko SY, Kong WP, Roychoudhuri R, Shi W, Bao S, Todd JP, Asmal M, Shen L, Donaldson M, Schmidt SD, Gall JG, Pinschewer DD, Letvin NL, Rao S, Mascola JR, Roederer M, Nabel GJ.** 2012. Gene-based vaccination with a mismatched envelope protects against simian immunodeficiency virus infection in nonhuman primates. J. Virol. 86:7760–7770.
9. **Thorner AR, Barouch DH.** 2007. HIV-1 vaccine development: progress and prospects. Curr. Infect. Dis. Rep. 9:71–75.
10. **McMichael AJ.** 2006. HIV vaccines. Annu. Rev. Immunol. 24:227–255.
11. **Burton DR, Poignard P, Stanfield RL, Wilson IA.** 2012. Broadly neutralizing antibodies present new prospects to counter highly antigenically diverse viruses. Science 337:183–186.
12. **D'Souza MP, Livnat D, Bradac JA, Bridges SH.** 1997. Evaluation of monoclonal antibodies to human immunodeficiency virus type 1 primary isolates by neutralization assays: performance criteria for selecting candidate antibodies for clinical trials. AIDS Clinical Trials Group Antibody Selection Working Group. J. Infect. Dis. 175:1056–1062.
13. **Scheid JF, Mouquet H, Feldhahn N, Seaman MS, Velinzon K, Pietzsch J, Ott RG, Anthony RM, Zebroski H, Hurley A, Phogat A, Chakrabarti B, Li Y, Connors M, Pereyra F, Walker BD, Wardemann H, Ho D, Wyatt RT, Mascola JR, Ravetch JV, Nussenzweig MC.** 2009. Broad diversity of neutralizing antibodies isolated from memory B cells in HIV-infected individuals. Nature 458:636–640.
14. **Walker LM, Phogat SK, Chan-Hui PY, Wagner D, Phung P, Goss JL, Wrin T, Simek MD, Fling S, Mitcham JL, Lehrman JK, Priddy FH, Olsen OA, Frey SM, Hammond PW, Kaminsky S, Zamb T, Moyle M, Koff WC, Poignard P, Burton DR.** 2009. Broad and potent neutralizing antibodies from an African donor reveal a new HIV-1 vaccine target. Science 326:285–289.
15. **Walker LM, Huber M, Doores KJ, Falkowska E, Pejchal R, Julien JP, Wang SK, Ramos A, Chan-Hui PY, Moyle M, Mitcham JL, Hammond PW, Olsen OA, Phung P, Fling S, Wong CH, Phogat S, Wrin T, Simek MD, Protocol GPI, Koff WC, Wilson IA, Burton DR, Poignard P.** 2011. Broad neutralization coverage of HIV by multiple highly potent antibodies. Nature 477:466–470.
16. **Huang J, Ofek G, Laub L, Louder MK, Doria-Rose NA, Longo NS, Imamichi H, Bailer RT, Chakrabarti B, Sharma SK, Alam SM, Wang T, Yang Y, Zhang B, Migueles SA, Wyatt R, Haynes BF, Kwong PD, Mascola JR, Connors M.** 2012. Broad and potent neutralization of HIV-1 by a gp41-specific human antibody. Nature 491:406–412.
17. **Zhou T, Georgiev I, Wu X, Yang ZY, Dai K, Finzi A, Kwon YD, Scheid JF, Shi W, Xu L, Yang Y, Zhu J, Nussenzweig MC, Sodroski J, Shapiro L, Nabel GJ, Mascola JR, Kwong PD.** 2010. Structural basis for broad and potent neutralization of HIV-1 by antibody VRC01. Science 329:811–817.
18. **McLellan JS, Pancera M, Carrico C, Gorman J, Julien JP, Khayat R, Louder R, Pejchal R, Sastry M, Dai K, O'Dell S, Patel N, Shahzad-ul Hussan S, Yang Y, Zhang B, Zhou T, Zhu J, Boyington JC, Chuang GY, Diwanji D, Georgiev I, Kwon YD, Lee D, Louder MK, Moquin S, Schmidt SD, Yang ZY, Bonsignori M, Crump JA, Kapiga SH, Sam NE, Haynes BF, Burton DR, Koff WC, Walker LM, Phogat S, Wyatt R, Orwenyo J, Wang LX, Arthos J, Bewley CA, Mascola JR, Nabel GJ, Schief WR, Ward AB, Wilson IA, Kwong PD.** 2011. Structure of HIV-1 gp120 V1/V2 domain with broadly neutralizing antibody PG9. Nature 480:336–343.
19. **Pejchal R, Doores KJ, Walker LM, Khayat R, Huang PS, Wang SK, Stanfield RL, Julien JP, Ramos A, Crispin M, Depetris R, Katpally U, Marozsan A, Cupo A, Maloveste S, Liu Y, McBride R, Ito Y, Sanders RW, Ogohara C, Paulson JC, Feizi T, Scanlan CN, Wong CH, Moore JP, Olson WC, Ward AB, Poignard P, Schief WR, Burton DR, Wilson IA.** 2011. A potent and broad neutralizing antibody recognizes and penetrates the HIV glycan shield. Science 334:1097–1103.
20. **Ryu SE, Hendrickson WA.** 2012. Structure and design of broadly-neutralizing antibodies against HIV. Mol. Cells 34:231–237.
21. **Stamatatos L, Morris L, Burton DR, Mascola JR.** 2009. Neutralizing antibodies generated during natural HIV-1 infection: good news for an HIV-1 vaccine? Nat. Med. 15:866–870.
22. **Saunders KO, Rudicell RS, Nabel GJ.** 2012. The design and evaluation of HIV-1 vaccines. AIDS 26:1293–1302.
23. **Haynes BF, Kelsoe G, Harrison SC, Kepler TB.** 2012. B-cell-lineage immunogen design in vaccine development with HIV-1 as a case study. Nat. Biotechnol. 30:423–433.
24. **Barouch DH, Liu J, Li H, Maxfield LF, Abbink P, Lynch DM, Iampietro MJ, SanMiguel A, Seaman MS, Ferrari G, Forthal DN, Ourmanov I, Hirsch VM, Carville A, Mansfield KG, Stablein D, Pau MG, Schuitemaker H, Sadoff JC, Billings EA, Rao M, Robb ML, Kim JH, Marovich MA, Goudsmit J, Michael NL.** 2012. Vaccine protection against acquisition of neutralization-resistant SIV challenges in rhesus monkeys. Nature 482:89–93.
25. **Kuwata T, Katsumata Y, Takaki K, Miura T, Igarashi T.** 2011. Isolation of potent neutralizing monoclonal antibodies from an SIV-Infected rhesus macaque by phage display. AIDS Res. Hum. Retroviruses 27:487–500.
26. **Kuwata T, Byrum R, Whitted S, Goeken R, Buckler-White A, Plishka R, Iyengar R, Hirsch VM.** 2007. A rapid progressor-specific variant clone of simian immunodeficiency virus replicates efficiently in vivo only in the absence of immune responses. J. Virol. 81:8891–8904.
27. **Kuwata T, Dehghani H, Brown CR, Plishka R, Buckler-White A, Igarashi T, Mattapallil J, Roederer M, Hirsch VM.** 2006. Infectious molecular clones from a simian immunodeficiency virus-infected rapid-progressor (RP) macaque: evidence of differential selection of RP-specific envelope mutations in vitro and in vivo. J. Virol. 80:1463–1475.
28. **Lusso P, Cocchi F, Balotta C, Markham PD, Louie A, Farci P, Pal R, Gallo RC, Reitz MS, Jr.** 1995. Growth of macrophage-tropic and primary

human immunodeficiency virus type 1 (HIV-1) isolates in a unique CD4+ T-cell clone (PM1): failure to downregulate CD4 and to interfere with cell-line-tropic HIV-1. J. Virol. 69:3712–3720.
29. Yusa K, Maeda Y, Fujioka A, Monde K, Harada S. 2005. Isolation of TAK-779-resistant HIV-1 from an R5 HIV-1 GP120 V3 loop library. J. Biol. Chem. 280:30083–30090.
30. Takeuchi Y, McClure MO, Pizzato M. 2008. Identification of gammaretroviruses constitutively released from cell lines used for human immunodeficiency virus research. J. Virol. 82:12585–12588.
31. Wei X, Decker JM, Liu H, Zhang Z, Arani RB, Kilby JM, Saag MS, Wu X, Shaw GM, Kappes JC. 2002. Emergence of resistant human immunodeficiency virus type 1 in patients receiving fusion inhibitor (T-20) monotherapy. Antimicrob. Agents Chemother. 46:1896–1905.
32. Derdeyn CA, Decker JM, Sfakianos JN, Wu X, O'Brien WA, Ratner L, Kappes JC, Shaw GM, Hunter E. 2000. Sensitivity of human immunodeficiency virus type 1 to the fusion inhibitor T-20 is modulated by coreceptor specificity defined by the V3 loop of gp120. J. Virol. 74:8358–8367.
33. Platt EJ, Wehrly K, Kuhmann SE, Chesebro B, Kabat D. 1998. Effects of CCR5 and CD4 cell surface concentrations on infections by macrophagetropic isolates of human immunodeficiency virus type 1. J. Virol. 72: 2855–2864.
34. DuBridge RB, Tang P, Hsia HC, Leong PM, Miller JH, Calos MP. 1987. Analysis of mutation in human cells by using an Epstein-Barr virus shuttle system. Mol. Cell. Biol. 7:379–387.
35. Hirsch V, Adger-Johnson D, Campbell B, Goldstein S, Brown C, Elkins WR, Montefiori DC. 1997. A molecularly cloned, pathogenic, neutralization-resistant simian immunodeficiency virus, SIVsmE543-3. J. Virol. 71: 1608–1620.
36. Kestler H, Kodama T, Ringler D, Marthas M, Pedersen N, Lackner A, Regier D, Sehgal P, Daniel M, King N, et al. 1990. Induction of AIDS in rhesus monkeys by molecularly cloned simian immunodeficiency virus. Science 248:1109–1112.
37. Mori K, Ringler DJ, Kodama T, Desrosiers RC. 1992. Complex determinants of macrophage tropism in env of simian immunodeficiency virus. J. Virol. 66:2067–2075.
38. Wu F, Ourmanov I, Kuwata T, Goeken R, Brown CR, Buckler-White A, Iyengar R, Plishka R, Aoki ST, Hirsch VM. 2012. Sequential evolution and escape from neutralization of simian immunodeficiency virus SIVsmE660 clones in rhesus macaques. J. Virol. 86:8835–8847.
39. Kuwata T, Nishimura Y, Whitted S, Ourmanov I, Brown CR, Dang Q, Buckler-White A, Iyengar R, Brenchley JM, Hirsch VM. 2009. Association of progressive CD4(+) T cell decline in SIV infection with the induction of autoreactive antibodies. PLoS Pathog. 5:e1000372. doi:10.1371/journal.ppat.1000372.
40. Barbas CF, Scott JM, Silverman G, Burton DR. 2001. Phage display: a laboratory manual. Cold Spring Harbor Laboratory Press, Cold Spring Harbor, NY.
41. Robinson JE, Holton D, Liu J, McMurdo H, Murciano A, Gohd R. 1990. A novel enzyme-linked immunosorbent assay (ELISA) for the detection of antibodies to HIV-1 envelope glycoproteins based on immobilization of viral glycoproteins in microtiter wells coated with concanavalin A. J. Immunol. Methods 132:63–71.
42. Kuwata T, Kodama M, Sato A, Suzuki H, Miyazaki Y, Miura T, Hayami M. 2007. Contribution of monocytes to viral replication in macaques during acute infection with simian immunodeficiency virus. AIDS Res. Hum. Retroviruses 23:372–380.
43. Matsumi S, Matsushita S, Yoshimura K, Javaherian K, Takatsuki K. 1995. Neutralizing monoclonal antibody against a external envelope glycoprotein (gp110) of SIVmac251. AIDS Res. Hum. Retroviruses 11:501–508.
44. Olshevsky U, Helseth E, Furman C, Li J, Haseltine W, Sodroski J. 1990. Identification of individual human immunodeficiency virus type 1 gp120 amino acids important for CD4 receptor binding. J. Virol. 64:5701–5707.
45. Walker LM, Simek MD, Priddy F, Gach JS, Wagner D, Zwick MB, Phogat SK, Poignard P, Burton DR. 2010. A limited number of antibody specificities mediate broad and potent serum neutralization in selected HIV-1 infected individuals. PLoS Pathog. 6:e1001028. doi:10.1371/journal.ppat.1001028.
46. Thali M, Moore JP, Furman C, Charles M, Ho DD, Robinson J, Sodroski J. 1993. Characterization of conserved human immunodeficiency virus type 1 gp120 neutralization epitopes exposed upon gp120-CD4 binding. J. Virol. 67:3978–3988.
47. Kent KA, Rud E, Corcoran T, Powell C, Thiriart C, Collignon C, Stott EJ. 1992. Identification of two neutralizing and 8 nonneutralizing epitopes on simian immunodeficiency virus envelope using monoclonal antibodies. AIDS Res. Hum. Retroviruses 8:1147–1151.
48. Hatada M, Yoshimura K, Harada S, Kawanami Y, Shibata J, Matsushita S. 2010. Human immunodeficiency virus type 1 evasion of a neutralizing anti-V3 antibody involves acquisition of a potential glycosylation site in V2. J. Gen. Virol. 91:1335–1345.
49. Yoshimura K, Shibata J, Kimura T, Honda A, Maeda Y, Koito A, Murakami T, Mitsuya H, Matsushita S. 2006. Resistance profile of a neutralizing anti-HIV monoclonal antibody, KD-247, that shows favourable synergism with anti-CCR5 inhibitors. AIDS. 20:2065–2073.
50. Lefranc MP, Giudicelli V, Ginestoux C, Jabado-Michaloud J, Folch G, Bellahcene F, Wu Y, Gemrot E, Brochet X, Lane J, Regnier L, Ehrenmann F, Lefranc G, Duroux P. 2009. IMGT, the international ImMunoGeneTics information system. Nucleic Acids Res. 37:D1006–D1012.
51. Gibbs RA, Rogers J, Katze MG, Bumgarner R, Weinstock GM, Mardis ER, Remington KA, Strausberg RL, Venter JC, Wilson RK, Batzer MA, Bustamante CD, Eichler EE, Hahn MW, Hardison RC, Makova KD, Miller W, Milosavljevic A, Palermo RE, Siepel A, Sikela JM, Attaway T, Bell S, Bernard KE, Buhay CJ, Chandrabose MN, Dao M, Davis C, Delehaunty KD, Ding Y, Dinh HH, Dugan-Rocha S, Fulton LA, Gabisi RA, Garner TT, Godfrey J, Hawes AC, Hernandez J, Hines S, Holder M, Hume J, Jhangiani SN, Joshi V, Khan ZM, Kirkness EF, Cree A, Fowler RG, Lee S, Lewis LR, Li Z, Liu YS, et al. 2007. Evolutionary and biomedical insights from the rhesus macaque genome. Science 316:222–234.
52. Tamura K, Peterson D, Peterson N, Stecher G, Nei M, Kumar S. 2011. MEGA5: molecular evolutionary genetics analysis using maximum likelihood, evolutionary distance, and maximum parsimony methods. Mol. Biol. Evol. 28:2731–2739.
53. Yokoyama M, Naganawa S, Yoshimura K, Matsushita S, Sato H. 2012. Structural dynamics of HIV-1 envelope Gp120 outer domain with V3 loop. PLoS One 7:e37530. doi:10.1371/journal.pone.0037530.
54. Huang C-c, Lam SN, Acharya P, Tang M, Xiang S-H, Hussan SS-u, Stanfield RL, Robinson J, Sodroski J, Wilson IA, Wyatt R, Bewley CA, Kwong PD. 2007. Structures of the CCR5 N terminus and of a tyrosine-sulfated antibody with HIV-1 gp120 and CD4. Science 317:1930–1934.
55. Chen X, Lu M, Poon BK, Wang Q, Ma J. 2009. Structural improvement of unliganded simian immunodeficiency virus gp120 core by normal-mode-based X-ray crystallographic refinement. Acta Crystallogr. D Biol. Crystallogr. 65:339–347.
56. Group W. 2005. GLYCAM web. Complex Carbohydrate Research Center, University of Georgia, Athens, GA.
57. Case DA, Cheatham TE, Darden T, Gohlke H, Luo R, Merz KM, Onufriev A, Simmerling C, Wang B, Woods RJ. 2005. The Amber biomolecular simulation programs. J. Comput. Chem. 26:1668–1688.
58. Pearlman DA, Case DA, Caldwell JW, Ross WS, Cheatham Iii TE, DeBolt S, Ferguson D, Seibel G, Kollman P. 1995. AMBER, a package of computer programs for applying molecular mechanics, normal mode analysis, molecular dynamics and free energy calculations to simulate the structural and energetic properties of molecules. Comput. Phys. Commun. 91:1–41.
59. Hornak V, Abel R, Okur A, Strockbine B, Roitberg A, Simmerling C. 2006. Comparison of multiple Amber force fields and development of improved protein backbone parameters. Proteins 65:712–725.
60. Kirschner KN, Yongye AB, Tschampel SM, González-Outeiriño J, Daniels CR, Foley BL, Woods RJ. 2008. GLYCAM06: a generalizable biomolecular force field. Carbohydrates. J. Comput. Chem. 29:622–655.
61. Jorgensen W, Chandrasekhar J, Madura J, Impey R, Klein M. 1983. Comparison of simple potential functions for simulating liquid water. J. Chem. Phys. 79:926–935.
62. Ryckaert J-P, Ciccotti G, Berendsen HJC. 1977. Numerical integration of the cartesian equations of motion of a system with constraints: molecular dynamics of n-alkanes. J. Comput. Physics 23:327–341.
63. Apetrei C, Kaur A, Lerche NW, Metzger M, Pandrea I, Hardcastle J, Falkenstein S, Bohm R, Koehler J, Traina-Dorge V, Williams T, Staprans S, Plauche G, Veazey RS, McClure H, Lackner AA, Gormus B, Robertson DL, Marx PA. 2005. Molecular epidemiology of simian immunodeficiency virus SIVsm in U.S. primate centers unravels the origin of SIVmac and SIVstm. J. Virol. 79:8991–9005.
64. Gorny MK, Wang XH, Williams C, Volsky B, Revesz K, Witover B, Burda S, Urbanski M, Nyambi P, Krachmarov C, Pinter A, Zolla-Pazner S, Nadas A. 2009. Preferential use of the VH5-51 gene segment by

the human immune response to code for antibodies against the V3 domain of HIV-1. Mol. Immunol. 46:917–926.
65. Yoshimura K, Harada S, Shibata J, Hatada M, Yamada Y, Ochiai C, Tamamura H, Matsushita S. 2010. Enhanced exposure of human immunodeficiency virus type 1 primary isolate neutralization epitopes through binding of CD4 mimetic compounds. J. Virol. 84:7558–7568.
66. Cole KS, Alvarez M, Elliott DH, Lam H, Martin E, Chau T, Micken K, Rowles JL, Clements JE, Murphey-Corb M, Montelaro RC, Robinson JE. 2001. Characterization of neutralization epitopes of simian immunodeficiency virus (SIV) recognized by rhesus monoclonal antibodies derived from monkeys infected with an attenuated SIV strain. Virology 290: 59–73.
67. Glamann J, Burton DR, Parren PW, Ditzel HJ, Kent KA, Arnold C, Montefiori D, Hirsch VM. 1998. Simian immunodeficiency virus (SIV) envelope-specific Fabs with high-level homologous neutralizing activity: recovery from a long-term-nonprogressor SIV-infected macaque. J. Virol. 72:585–592.
68. Edinger AL, Ahuja M, Sung T, Baxter KC, Haggarty B, Doms RW, Hoxie JA. 2000. Characterization and epitope mapping of neutralizing monoclonal antibodies produced by immunization with oligomeric simian immunodeficiency virus envelope protein. J. Virol. 74:7922–7935.
69. Zhang PF, Cham F, Dong M, Choudhary A, Bouma P, Zhang Z, Shao Y, Feng YR, Wang L, Mathy N, Voss G, Broder CC, Quinnan GV, Jr. 2007. Extensively cross-reactive anti-HIV-1 neutralizing antibodies induced by gp140 immunization. Proc. Natl. Acad. Sci. U. S. A. 104:10193–10198.
70. Huang C-c, Venturi M, Majeed S, Moore MJ, Phogat S, Zhang M-Y, Dimitrov DS, Hendrickson WA, Robinson J, Sodroski J, Wyatt R, Choe H, Farzan M, Kwong PD. 2004. Structural basis of tyrosine sulfation and VH-gene usage in antibodies that recognize the HIV type 1 coreceptor-binding site on gp120. Proc. Natl. Acad. Sci. U. S. A. 101:2706–2711.
71. Xiao X, Chen W, Feng Y, Zhu Z, Prabakaran P, Wang Y, Zhang MY, Longo NS, Dimitrov DS. 2009. Germline-like predecessors of broadly neutralizing antibodies lack measurable binding to HIV-1 envelope glycoproteins: implications for evasion of immune responses and design of vaccine immunogens. Biochem. Biophys. Res. Commun. 390:404–409.
72. Chen W, Streaker ED, Russ DE, Feng Y, Prabakaran P, Dimitrov DS. 2012. Characterization of germline antibody libraries from human umbilical cord blood and selection of monoclonal antibodies to viral envelope glycoproteins: implications for mechanisms of immune evasion and design of vaccine immunogens. Biochem. Biophys. Res. Commun. 417: 1164–1169.
73. Robinson JE, Franco K, Elliott DH, Maher MJ, Reyna A, Montefiori DC, Zolla-Pazner S, Gorny MK, Kraft Z, Stamatatos L. 2010. Quaternary epitope specificities of anti-HIV-1 neutralizing antibodies generated in rhesus macaques infected by the simian/human immunodeficiency virus SHIVSF162P4. J. Virol. 84:3443–3453.
74. Yuan T, Li J, Zhang Y, Wang Y, Streaker E, Dimitrov DS, Zhang M-Y. 2011. Putative rhesus macaque germline predecessors of human broadly HIV-neutralizing antibodies: differences from the human counterparts and implications for HIV-1 vaccine development. Vaccine 29:6903–6910.
75. Link JM, Larson JE, Schroeder HW. 2005. Despite extensive similarity in germline DH and JH sequence, the adult rhesus macaque CDR-H3 repertoire differs from human. Mol. Immunol. 42:943–955.
76. Labrijn AF, Poignard P, Raja A, Zwick MB, Delgado K, Franti M, Binley J, Vivona V, Grundner C, Huang Venturi C-CM, Petropoulos CJ, Wrin T, Dimitrov DS, Robinson J, Kwong PD, Wyatt RT, Sodroski J, Burton DR. 2003. Access of antibody molecules to the conserved coreceptor binding site on glycoprotein gp120 is sterically restricted on primary human immunodeficiency virus type 1. J. Virol. 77:10557–10565.
77. Thenin S, Roch E, Samleerat T, Moreau T, Chaillon A, Moreau A, Barin F, Braibant M. 2012. Naturally occurring substitutions of conserved residues in human immunodeficiency virus type 1 variants of different clades are involved in PG9 and PG16 resistance to neutralization. J. Virol. 93: 1495–1505.
78. Utachee P, Nakamura S, Isarangkura-Na-Ayuthaya P, Tokunaga K, Sawanpanyalert P, Ikuta K, Auwanit W, Kameoka M. 2010. Two N-linked glycosylation sites in the V2 and C2 regions of human immunodeficiency virus type 1 CRF01_AE envelope glycoprotein gp120 regulate viral neutralization susceptibility to the human monoclonal antibody specific for the CD4 binding domain. J. Virol. 84:4311–4320.
79. Henzler-Wildman K, Kern D. 2007. Dynamic personalities of proteins. Nature 450:964–972.
80. Ode H, Nakashima M, Kitamura S, Sugiura W, Sato H. 2012. Molecular dynamics simulation in virus research. Front. Microbiol. 3:258.
81. Klein F, Gaebler C, Mouquet H, Sather DN, Lehmann C, Scheid JF, Kraft Z, Liu Y, Pietzsch J, Hurley A, Poignard P, Feizi T, Morris L, Walker BD, Fatkenheuer G, Seaman MS, Stamatatos L, Nussenzweig MC. 2012. Broad neutralization by a combination of antibodies recognizing the CD4 binding site and a new conformational epitope on the HIV-1 envelope protein. J. Exp. Med. 209:1469–1479.
82. Poignard P, Saphire EO, Parren PW, Burton DR. 2001. GP120: biologic aspects of structural features. Annu. Rev. Immunol. 19:253–274.
83. Sekaly RP. 2008. The failed HIV Merck vaccine study: a step back or a launching point for future vaccine development? J. Exp. Med. 205:7–12.
84. Watkins DI, Burton DR, Kallas EG, Moore JP, Koff WC. 2008. Nonhuman primate models and the failure of the Merck HIV-1 vaccine in humans. Nat. Med. 14:617–621.

Journal of General Virology (2013), 94, 933–943 DOI 10.1099/vir.0.047167-0

Impact of antiretroviral pressure on selection of primary human immunodeficiency virus type 1 envelope sequences *in vitro*

Shigeyoshi Harada,[1,2] Kazuhisa Yoshimura,[1,2] Aki Yamaguchi,[1] Samatchaya Boonchawalit,[1,2] Keisuke Yusa[3] and Shuzo Matsushita[1]

Correspondence
Kazuhisa Yoshimura
ykazu@nih.go.jp

[1]Center for AIDS Research, Kumamoto University, 2-2-1 Honjo, Chuo-ku, Kumamoto 860-0811, Japan

[2]AIDS Research Center, National Institute of Infectious Diseases, 1-23-1 Toyama, Shinjuku-ku, Tokyo 162-8640, Japan

[3]Division of Biological Chemistry and Biologicals, National Institute of Health Sciences, 1-18-1 Kami-youga, Setagaya-ku, Tokyo 158-8501, Japan

The initiation of drug therapy results in a reduction in the human immunodeficiency virus type 1 (HIV-1) population, which represents a potential genetic bottleneck. The effect of this drug-induced genetic bottleneck on the population dynamics of the envelope (Env) regions has been addressed in several *in vivo* studies. However, it is difficult to investigate the effect on the *env* gene of the genetic bottleneck induced not only by entry inhibitors but also by non-entry inhibitors, particularly *in vivo*. Therefore, this study used an *in vitro* selection system using unique bulk primary isolates established in the laboratory to observe the effects of the antiretroviral drug-induced bottleneck on the integrase and *env* genes. Env diversity was decreased significantly in one primary isolate [KP-1, harbouring both CXCR4 (X4)- and CCR5 (R5)-tropic variants] when passaged in the presence or absence of raltegravir (RAL) during *in vitro* selection. Furthermore, the RAL-selected KP-1 variant had a completely different Env sequence from that in the passage control (particularly evident in the gp120, V1/V2 and V4-loop regions), and a different number of potential *N*-glycosylation sites. A similar pattern was also observed in other primary isolates when using different classes of drugs. This is the first study to explore the influence of anti-HIV drugs on bottlenecks in bulk primary HIV isolates with highly diverse Env sequences using *in vitro* selection.

Received 15 August 2012
Accepted 20 December 2012

INTRODUCTION

Human immunodeficiency virus type 1 (HIV-1) shows a high degree of genetic diversity owing to its high rates of replication and recombination and the high mutation rate of the HIV-1 reverse transcriptase (Nájera *et al.*, 2002). Even in a single infected individual, the virus can best be described as a population of distinct, but closely related, genetic variants or 'quasi-species' (Eigen, 1993; Nijhuis *et al.*, 1998). The quasi-species behaviour of viruses is recognized as a key element in our understanding and modelling of viral evolution and disease control (Vignuzzi *et al.*, 2006).

Combination antiretroviral (ARV) therapy results in a contraction of the viral population, which represents a potential genetic bottleneck (Charpentier *et al.*, 2006; Delwart *et al.*, 1998; Ibáñez *et al.*, 2000; Kitrinos *et al.*, 2005; Nijhuis *et al.*, 1998; Nora *et al.*, 2007; Sheehy *et al.*, 1996; Zhang *et al.*, 1994). Whilst this bottleneck has a direct effect on the region that is being targeted by the drugs (e.g. protease or reverse transcriptase), it also affects other regions of the viral genome. Indeed, the effect of the drug-induced genetic bottleneck on the population dynamics of the envelope (Env) regions has been addressed in several *in vivo* studies (Charpentier *et al.*, 2006; Delwart *et al.*, 1998; Ibáñez *et al.*, 2000; Kitrinos *et al.*, 2005; Nijhuis *et al.*, 1998; Nora *et al.*, 2007; Sheehy *et al.*, 1996; Zhang *et al.*, 1994).

Virus bottleneck evolution of the HIV-1 *env* gene might be important when choosing the optimal drugs to treat a particular patient. Indeed, a CCR5 antagonist (maraviroc, MVC) and a fusion inhibitor (enfuvirtide, T-20) have now

The GenBank/EMBL/DDBJ accession numbers for the *env* sequences of HIV-1 KP-1, KP-2 and KP-4, are AB640872–AB640881, AB641341–AB641351 and AB641335–AB641340, respectively.

Two supplementary figures are available with the online version of this paper.

been approved for use as HIV-1 entry inhibitors. Analysing the dynamics of drug-induced genetic bottlenecks and studying drug-resistant mutation profiles in response to HIV-1-specific ARV drugs are both important if we are to understand fully HIV-1 drug resistance and pathogenesis.

The aim of the present study was to understand better the effect of *in vivo* drug-induced genetic bottlenecks. *In vitro* selection of different primary HIV-1 isolates was performed using the recently approved HIV integrase inhibitor raltegravir (RAL) (Steigbigel *et al.*, 2008). Two R5-, one X4-, one dual- and one mixed R5/X4-tropic isolates were passaged through a RAL-induced genetic bottleneck. We also performed *in vitro* selection of the R5/X4 isolate using lamivudine (3TC), saquinavir (SQV) and MVC, and compared the results with those from the RAL-selected isolate.

RESULTS

Genotypic profiles of the HIV-1 primary isolates

Four genetically heterogeneous HIV-1 primary isolates (KP-1–4) from Japanese drug-naïve patients were used to assess the extent to which RAL affected the selection of bulk primary viruses *in vitro*. A laboratory isolate, strain 89.6, was also used in the study (rather than a molecular clone) to allow escape mutants to be selected from each quasi-species pool and to be generated *de novo*. First, the sequences of the integrase (IN) regions of the four primary isolates were determined. Table 1 shows the detailed evaluation of the R5/X4 mixture subtype B (KP-1), R5-CRF08_BC (KP-2), R5 subtype B (KP-3) and X4-CRF01_AE (KP-4) primary isolates, and the dual-tropic subtype B laboratory virus (89.6). Although some naturally occurring polymorphisms were observed within the IN regions of these isolates compared with the subtype B consensus sequence available from the Los Alamos National Laboratory HIV sequence database, we did not identify any primary resistant mutations to RAL. Three baseline viruses (KP-1, KP-4 and 89.6) were sensitive to RAL, with IC_{50} values ranging from 1.2 to 4 nM, which are comparable with those reported previously (Kobayashi *et al.*, 2008). However, KP-2 and KP-3 showed minor resistance to RAL, with IC_{50} values of 16 and 32 nM, respectively. These two isolates contained amino acid mutations at positions 72, 125 and 201 within the IN region [previously reported as L-870,810 and S-1360 resistance mutations (Hombrouck *et al.*, 2008; Rhee *et al.*, 2008), but not as RAL-resistance mutations]. KP-2 also contained a unique insertion at position 288 (NQDME) at the C-terminal end of the IN region.

In vitro selection of variants of the primary isolates and 89.6 using RAL

To induce RAL-selected HIV-1 variants *in vitro*, PM1/CCR5 cells, a T-cell line expressing high levels of CCR5, were exposed to the four primary isolates and strain 89.6. The viruses were then serially passaged in the presence of RAL. As a control, each isolate was passaged under the same conditions, but without RAL, to allow monitoring of spontaneous changes occurring in the viruses during prolonged PM1/CCR5 cell passage (the passage control). The selected viruses were initially propagated at a RAL concentration equal to each IC_{50} value. The RAL concentrations were then increased from 20 to 85 nM during the course of the selection procedure (Table 1).

Only small shifts in the IC_{50} to RAL were observed in four of the five isolates (KP-1, KP-2, KP-4 and 89.6), with fold changes in IC_{50} values of 3.4, 6.5, 16 and 9.2, respectively. KP-3 did not show resistance to RAL. IC_{50} values in all the passage controls were comparable with those of the baseline viruses (Table 1).

IN region sequences in RAL-selected variants

The full-length *IN* genes were amplified and cloned to determine the genetic basis of selection in the presence or absence of RAL. Ten to 12 clones from each sample were sequenced.

Substitutions within IN were observed at passages 30 (G189R) and 29 (T210I) in two RAL-selected isolates (KP-2 and KP-4, respectively). Neither of these has been reported as IN inhibitor-resistant mutations. No substitutions in the IN regions of KP-3 and 89.6 were found. However, A125T and V180I substitutions were observed in the KP-3 and 89.6 control variants at the last passage. No previously reported mutations were identified in the IN region of KP-1 (an R5/X4 mixture isolate) after 17 passages. However, four amino acids (K7/K111/H216/D278) were selected by RAL from the baseline quasi-species, whereas different amino acids (R7/R111/Q216/N278) were selected in the control-passage variants (Table 1).

Taken together, these findings showed that RAL-induced selection pressure causes adaptation within the IN regions of bulk primary viruses during *in vitro* passage in the target cells, and confirmed that this system can be used to analyse drug-selected variants *in vitro*.

Comparison of *env* gene sequences in RAL-selected and passage-control isolates

A highly diverse gp120 region was observed in the baseline R5/X4 mixture isolate, KP-1; however, the viral diversity of variants passaged in the presence or absence of RAL decreased significantly during *in vitro* selection (overall mean distance after RAL selection of 0.056 at baseline to 0.007 after passage 17; mean overall distance in the passage control of 0.01 after 20 passages, Table 2). Moreover, the RAL-selected and control variants utilized CCR5 to enter the target cell; neither variant used CXCR4 (Table 3).

Interestingly, the low-diversity RAL-selected variant contained a completely different Env sequence from that of the passage-control variant (Fig. 1a). Different regions spanning

Table 1. Susceptibility of HIV-1 isolates to RAL and distinct differences in IN region sequences between RAL-selected and control-passaged viruses

Isolate	Subtype	Tropism	Passage no.	Concn (nM)	RAL-selected variant*		Passage control	
					IN sequence	RAL IC_{50} (nM)	IN sequence	RAL IC_{50} (nM)
KP-1	B	Mix	0	0	*K/R7, K/R111, Q/H216, D/N278*	4	*K/R7, K/R111, Q/H216, D/N278*	4
			8	20	**K**111, **H**216, **D**278	31 (7.8)	**R**7, **R**111, **Q**216, **N**278	4.5 (1.2)
			17†	20	**K**7, **K**111, **H**216, **D**278	26 (6.5)	**R**7, **R**111, **Q**216, **N**278	0.4 (0.1)
KP-2	CRF08_BC	R5	0	0	*I201, ins289NQDME*	16	*I201, ins289NQDME*	16
			18	40	G189G/R, *I201, ins289NQDME*	32 (2)	*I201, ins289NQDME*	16 (1)
			30	85	G189R, *I201, ins289NQDME*	55 (3.4)	*I201, ins289NQDME*	25 (1.6)
KP-3	B	R5	0	0	*V72, A125*	32	*V72, A125*	32
			11	25	*V72, A125*	25 (0.78)	*V72, A125*	33 (1)
			22	27.5	*V72, A125*	37 (1.2)	*V72,* A125T	13 (0.41)
KP-4	CRF01_AE	X4	0	0	–	2.1	–	2.1
			8	40	–	33 (16)	R166R/K, D279N	4.4 (2.1)
			29	40	T210I	22 (10)	G163E, R166R/K, D279N/S	4.1 (2)
89.6	B	R5X4	0	0	–	1.2	–	1.2
			8	15	–	34 (28)	–	4.4 (3.7)
			34	20	–	11 (9.2)	V180I	1.2 (1)

*Amino acid changes in each passage variant are shown. Italicized letters represent mutations relative to the consensus subtype BC or B present in the baseline isolates. Bold letters represent amino acids selected out of the quasi-species cloud. The fold increase in RAL IC_{50} values is shown in parentheses for *in vitro*-selected variants compared with those in the baseline isolates.
†The RAL variant selected after 17 passages was compared with the control selected after 20 passages.

Table 2. Comparison of amino acid length and number of PNGs between RAL-selected and control-passage KP-1 variants

	Passage no.	Genetic diversity*	Mean ENV $_{1-474}$ length (range)†	Mean V1/V2 length (range)	Mean V3 length (range)	Mean V4 length (range)	Mean PNGs (range)
Baseline	0	0.056	472 (461–480)	69 (60–74)	34 (33–34)	30 (29–31)	24 (22–28)
RAL-selected virus	2	0.038	479 (472–480)‡	74 (71–74)‡	34 (33–34)‡	31 (29–31)‡	27 (25–28) ‡
	8	0.0070	480	74	34	31	28 (26–29)
	17	0.0070	480	74	34	31	27 (26–27)§
Passage control	2	0.045	464 (461–466)‡	64 (60–74)‡	34 (33–34)‡	29 (29–31)‡	24 (22–27)‡
	8	0.0070	463 (462–463)	62	34	29	23 (22–23)
	10	0.0080	462 (459–463)	62	34	29	23 (22–23)
	20	0.010	463	62	34	29	23 (22–23)§
P value			<0.0001‡	<0.0001‡	0.91‡	0.0048‡	0.0019‡ <0.0001§

*Overall mean distance.
†Sequence from gp120 SP to the V5 region (aa 1–474).
‡, § *P* values were calculated using the homoscedastic *t*-test between the RAL-selected and the passage-control variants indicated by the same symbols above.

the whole envelope sequence [from the signal peptide (SP) to V5] were compared in the RAL-selected and passage-control viruses. The results showed that, after only two passages, the gp120, V1/V2 and V4-loop regions within RAL-selected variants were longer than those in the control variants, and the number of putative *N*-linked glycosylation sites (PNGs) was significantly higher than that in the control-passage viruses (Table 2). This phenomenon was seen consistently in two independent experiments.

We also analysed the gp120 sequences in the other four isolates. Although the number of positional differences between the RAL-selected and passage-control variants for these four isolates was lower than that in KP-1 (between three and nine, compared with >40), there was a similar pattern of separation between the Env sequences (Fig. 1). In three of the four isolates (KP-2, KP-3 and KP-4), positional differences were observed in SP, C1 and all the variable regions of gp120 (Fig. 1b–d). In strain 89.6, differences were observed in the C2, C3 and V4 regions (Fig. 1e).

These results suggested that RAL treatment of target cells causes a decrease in viral diversification within quasi-species Env regions via a route different from that in untreated target cells.

In vitro induction of RAL-selected V3-loop library virus variants

To investigate further the effects of RAL on viral Env sequences, we used the V3-loop library virus (JR-FL-V3Lib) developed by Yusa *et al.* (2005), which carries a set of random combinations from zero to ten substitutions (27 648 possibilities) in the V3 loop (residues 305, 306, 307, 308, 309, 317, 319, 322, 323 and 326; V3 loop from Cys^{296} to Cys^{331}). The variants contained in the library were polymorphic mutations derived from 31 R5 clinical isolates (Yusa *et al.*, 2005). PM1/CCR5 cells were exposed to the JR-FL-V3Lib and serially passaged in the presence of RAL. After two passages, the V3 sequence within the RAL-selected variant was completely different from that in the passage control (Fig. 1f). This suggested that, under pressure from RAL, the infectious clone harbouring different V3 region sequence from the passage control had adapted to the target cells, despite containing the same IN sequences.

Phylogenetic analysis of the Env regions after passage with or without RAL

To confirm the temporal and spatial differences observed in each of the RAL-selected and passage-control viruses, phylogenetic analyses were conducted using complete SP–V5 sequences. The neighbour-joining phylogenetic tree showed a clear and distinct branching between RAL-selected and passage-control KP-1 viruses (Fig. 2a). We also identified a similar pattern in all the other isolates tested (Fig. 2b–e).

Table 3. Comparison of amino acid length, number of potential *N*-linked glycosylation sites, V3 sequences and co-receptor usage between anti-retroviral drug-selected and control-passaged KP-1 variants

	Passage no.	Genetic diversity*	Mean ENV_{1-474} length (range)†	Mean V1/V2 length (range)	Mean V3 length (range)	Mean V4 length (range)	Mean PNGs (range)	V3 region		Geno2 pheno (%)§
								Prevalence (%)	Sequence‡	
Baseline	0	0.056	472 (461–480)	69 (60–74)	34 (33–34)	30 (29–31)	24 (22–28)	41.9	CTRPNNNTRKGIHIGPGKFYATGAIIGDIRQAHC	41.2
								22.6	.....V.....	41.2
								16.1	....-..I.....T.R..T.RD...N..K...	1.7
								13.0	....-..I.....T.R..T.KT...N.KK...	2.9
								3.2	....-..I.....	7.4
								3.2	.....D.....	55.3
Passage control	8	0.0070	463 (462–463)	62	34	29	23 (22–23)	100.0	.....V.....	41.2
RAL-selected virus	8	0.0070	480	74	34	31	28 (26–29)	100.0	.....	41.2
3TC-selected virus	6	0.020	478 (475–480)	74	34	31 (29–31)	27 (25–28)	83.3	.....	41.2
SQV-selected virus	11	0.0040	474	71	34	31	26	100.0	.....	41.2
MVC-selected virus	7	0.0080	469 (468–469)	69	33	29	24 (23–24)	100.0	....-..I....R..T.R..T.KT...N.KK...	1.7

*Overall mean distance.

†Sequence from gp120 SP to the V5 region (aa 1–474).

‡V3 sequences of each variant are shown. Dots denote sequence identity and dashes indicate a deletion mutation.

§Prediction of viral co-receptor tropism using Geno2pheno based on a selectable 'false positive rate'.

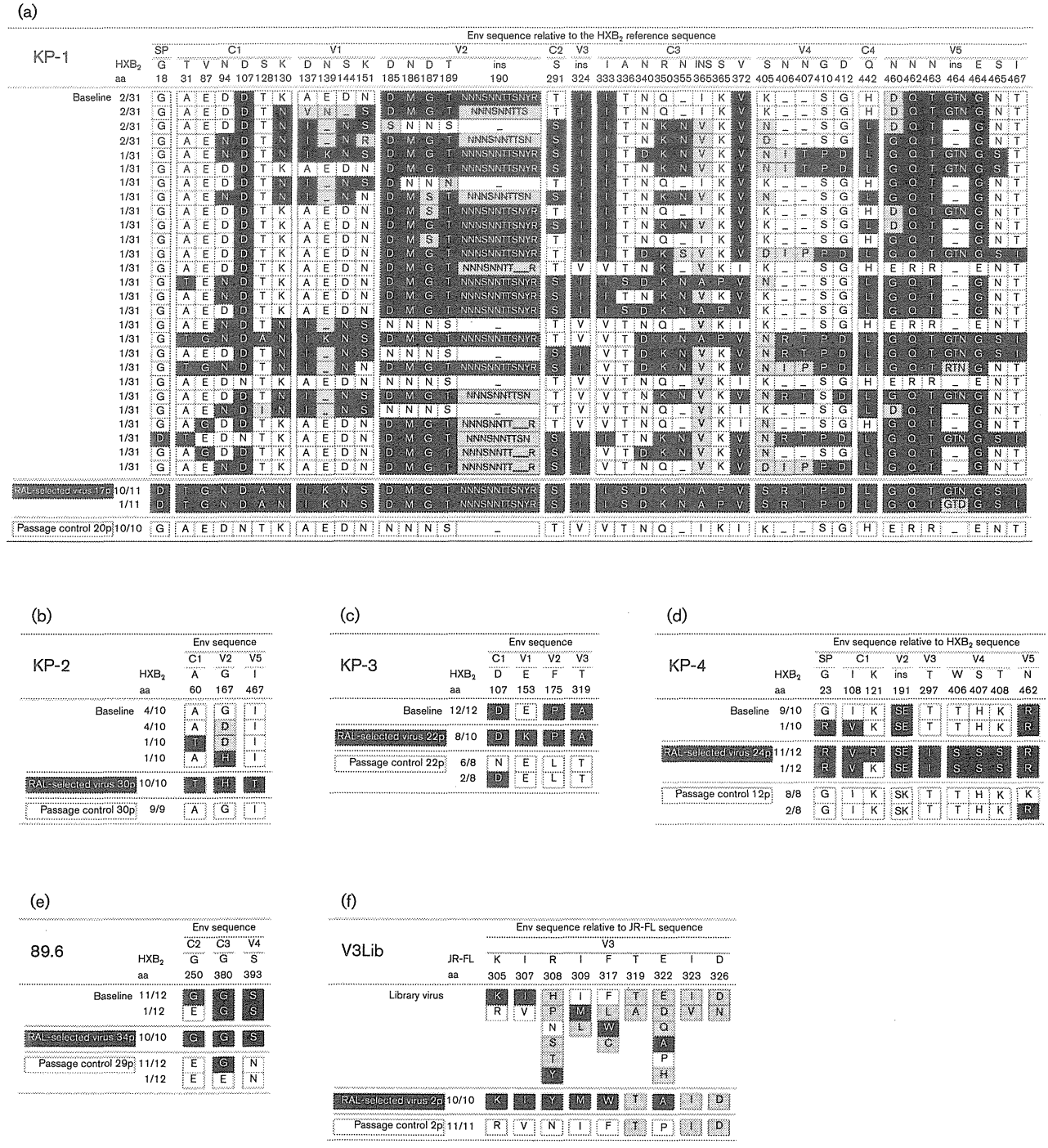

Fig. 1. Comparison of the gp120 sequences between RAL-selected and control-passaged viruses. The gp120 sequences of baseline, RAL-selected and the passage-control viruses were aligned for KP-1 (a), KP-2 (b), KP-3 (c), KP-4 (d) and strain 89.6 (e). Each amino acid in (a)–(e) is numbered relative to the HIV-1 HXB_2 reference sequence. The V3 sequences from the JR-FL-V3Lib baseline library, RAL-selected and passage-control viruses were aligned (f). Filled cells denote the most dominant amino acids observed in RAL-selected variants at the latest passage, open cells denote the most dominant amino acids observed in the passage-control variants at the latest passage and shaded cells show amino acids deleted by the end of both passages, whilst '–' indicates a deletion mutation. The number of passages is indicated, e.g. 17p for passage 17.

In vitro selection of KP-1 variants by 3TC, SQV and MVC

To determine whether other HIV drugs also changed the route of adaptation to the target cells, we attempted to select KP-1 variants using a reverse transcriptase inhibitor (3TC), a protease inhibitor (SQV) and a CCR5 inhibitor (MVC). As shown in Fig. 2(f), the pattern of clustering at distinct positions between the selected isolates and the passage-control variants was similar to that observed for the RAL-selected variants. The selected variants showed decreased diversity in the gp120 sequences; however, the length of the gp120, V1/V2 and V4 sequences increased (apart from in the MVC-selected variants). In addition, the number of PNGs within gp120 was higher than that in the control (Table 3). We also compared the V3 sequences between the passage-control and each of the drug-selected variants. The V3 sequences in all the SQV-selected variants and 83.3 % of those in the 3TC-selected variants, were comparable with those in the RAL-selected variants. This was not the case for the passage controls. Comparison of variants passaged with RAL and 3TC showed that the length of the V1/V2 and V4 regions and the number of PNGs was similar; however, these parameters were different in the SQV-selected variants (Table 3). This indicated that the time at which a drug acts (e.g. during the early or late phase of the HIV life cycle) influences the selection of Env sequences. During selection with MVC, CXCR4-tropic variants were selected from the baseline mixture after seven passages.

Taken together, these results suggested that, in treated cells, different classes of anti-HIV drugs may suppress the variability of quasi-species during *in vitro* selection via a route different from that in untreated cells.

DISCUSSION

This study evaluated the impact of anti-HIV drugs on the Env bottleneck in bulk HIV-1 primary isolates during selection *in vitro*. RAL-, 3TC- and SQV-selected variants of the unique viral isolate, KP-1, harbouring both X4 and R5 variants and with a very high level of baseline viral diversity, were used to study the final destination (genetic bottleneck) of a large variety of Env sequences. Interestingly, the phylogenetic clustering of RAL-selected KP-1 variants was completely different from that of non-drug-treated controls (Fig. 2). Our results also confirmed differences in the length of the gp120, V1/V2 and V4-loop regions and in the number of PNGs (Tables 2 and 3).

It is not clear why viruses cultured under pressure from the non-Env-directed drug RAL result in different *env* genotypes compared with those without the drug. Thus, we cloned the *IN–env* region of the proviral genome from passaged viruses and sequenced the *env* and *IN* regions on the same cloned plasmid, and compared them among the baseline and passages 1, 2, 8 and 17 of the KP-1 virus. Under low concentrations of the IN inhibitor RAL, K7 was selected for at a late passage after accumulation of the other three amino acids, K111, D278 and H216, in IN. During the sequential accumulation of these four amino acids (K111, D278, H216 and K7), the RAL-selected Env sequences at passage 17 (the Env sequences shown as filled boxes in Fig. 1) sequentially accumulated mutations in the same proviral genome (Fig. S1, available in JGV Online). However, we did not find a clone including both the RAL-selected Env at passage 17 and RAL-selected IN at passage 17 in the baseline or each passaged virus, except for in the last passage. We also examined the gp120 and IN sequences of the 3TC- and SQV-selected KP-1 variants. Compared with the RAL-selected region, the variable regions of gp120 in these selected variants were very similar to each other, except for the V1/V2 region (Fig. S2). However, the passage-control variant was very different from the drug-selected variants (Fig. 1a). Furthermore, the IN sequences were different in each passaged virus: K111/D278/H216/K7 in RAL-selected, R111/D278/Q216/R7 in 3TC-selected, K111/D278/H216/R7 in SQV-selected and R111/N278/Q216/R7 in virus without drug treatment (underlined residues indicate amino acids different from those in viruses without drug treatment). To explain these results, we believe that, under pressure from anti-HIV drugs (non-entry ARVs), the virus might show a primitive reaction to select for the Env sequence and recombine from quasi-species to gain advantage for entry and/or enhance replication in target cells. Meanwhile, IN was selected from quasi-species by a direct and/or indirect effect of RAL-induced pressure. The combination of both selective pressures may affect the selection for Env and IN during adaptation in drug-treated conditions (Figs 1a and S2). These results suggest that non-entry inhibitors, such as RAL, 3TC and SQV, might also affect cell adaptation to PM1/CCR5 cells.

Many *in vivo* studies have reported the effects of the anti-HIV drug-induced bottleneck on the *env* gene (Charpentier *et al.*, 2006; Delwart *et al.*, 1998; Ibáñez *et al.*, 2000; Kitrinos *et al.*, 2005; Nijhuis *et al.*, 1998; Nora *et al.*, 2007; Sheehy *et al.*, 1996; Zhang *et al.*, 1994). However, these studies had several limitations. Because viruses were placed under *in vivo* selective pressure using at least two anti-HIV drugs and by the host immune response, it is difficult to separate the different effects and to draw clear conclusions, particularly *in vivo*. Delwart *et al.* (1998) and Kitrinos *et al.* (2005) avoided some of these limitations by employing a heteroduplex tracking assay, although *in vivo* peculiarities still remained. Therefore, we used an *in vitro* selection system using unique bulk primary isolates established in our laboratory (Hatada *et al.*, 2010; Shibata *et al.*, 2007; Yoshimura *et al.*, 2006, 2010b) to observe the effects of the anti-retroviral drug-induced bottleneck on the *IN* and *env* genes.

This selection provides a sensitive approach for analysing virus population dynamics. The effectiveness of ARV drugs can be examined during the *in vitro* passage of a single variant or mixture of variants without being affected by many of the factors encountered *in vivo*. In addition,

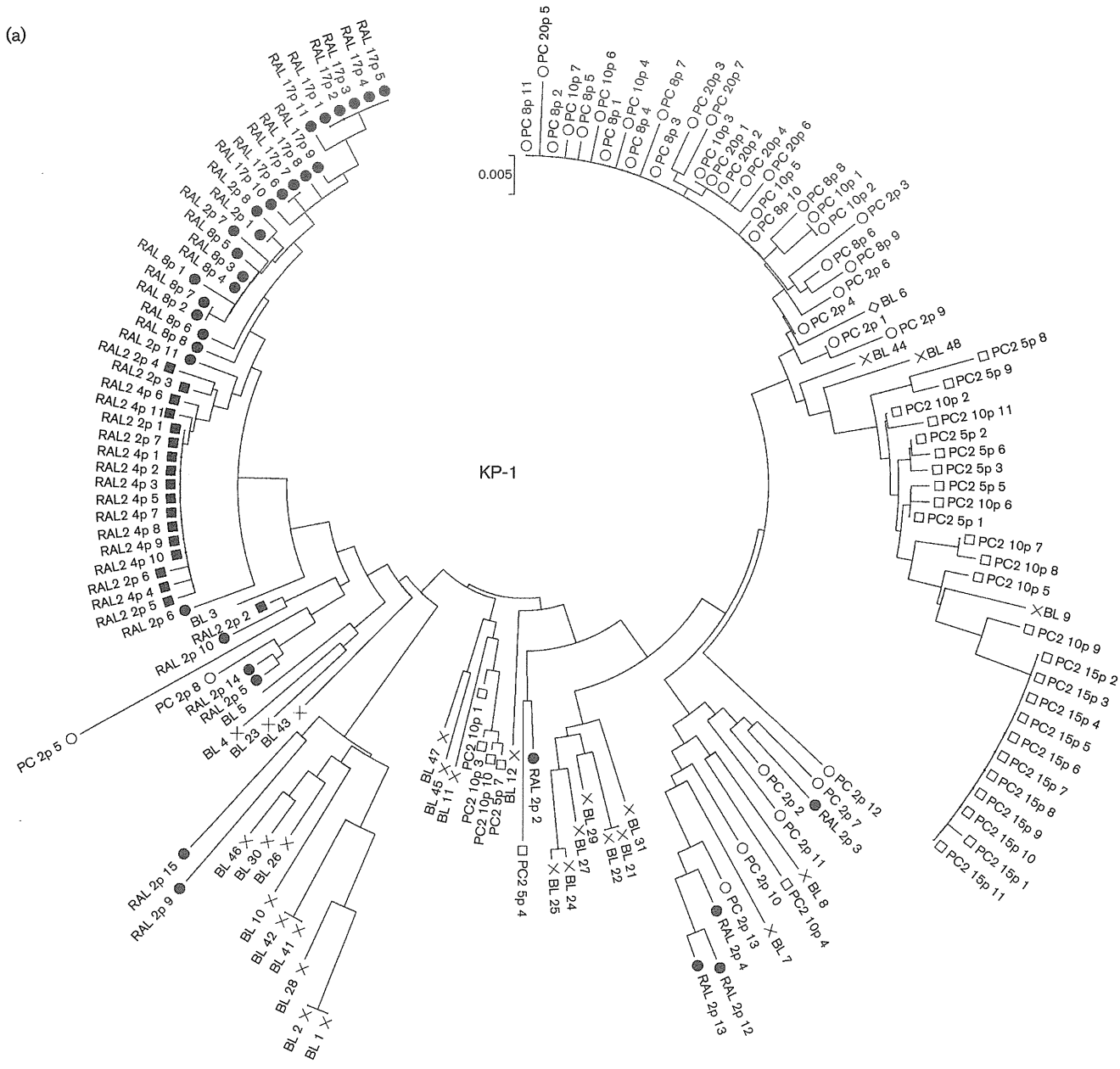

Fig. 2. Phylogenetic analyses of the Env regions from *in vitro*-passaged viruses selected with or without ARV drugs. (a–e) Phylogenetic trees were constructed using gp120 SP–V5 sequences from RAL-selected and passage-control variants of KP-1 (a), KP-2 (b), KP-3 (c), KP-4 (d) and strain 89.6 (e). An '×' represents baseline (BL) variants, and closed and open symbols represent RAL-selected (RAL) and passage-control (PC) variants, respectively. In (a), the results of the second experiment are indicated as RAL2 and PC2, respectively. (f) A phylogenetic tree was constructed using gp120 SP–V5 sequences from RAL-, 3TC-, SQV-, MVC-selected and control-passaged variants of KP-1. ○, Control variants after eight passages; ●, RAL-selected variants after eight passages; ▲, 3TC-selected variants after six passages; ◆, SQV-selected variants after 11 passages; ■, MVC-selected variants after seven passages. The trees were constructed using the neighbour-joining algorithm embedded within the MEGA software.

differences in the Env sequences between the baseline and selected variants can be compared after any number of passages. The results of the present study provide important information that will enhance our understanding of the drug-induced genetic bottleneck. This phenomenon can be examined *in vitro* using bulk primary isolates treated with or without drugs.

Recently, several new ARV drugs have been licensed for use in HIV-1-infected patients. MVC, approved in 2006, is the

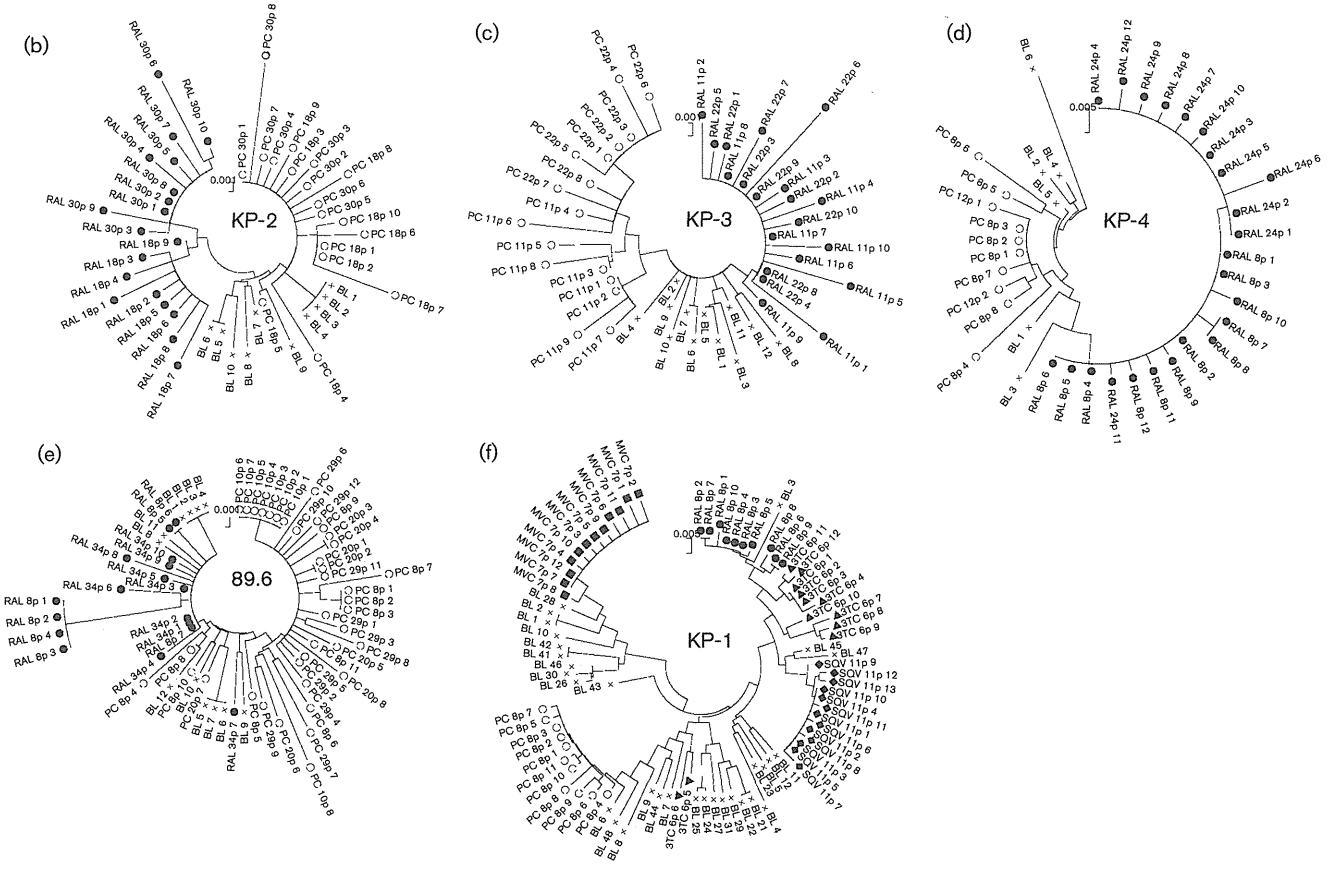

first CCR5 inhibitor (Gulick *et al.*, 2008). One important advantage associated with this drug is the absence of cross-resistance with previously available ARV compounds (Gulick *et al.*, 2008; Steigbigel *et al.*, 2008). However, as is usual with anti-HIV drugs, resistant variants with mutations in the Env, gp120 and gp41 sequences are induced both *in vivo* and *in vitro* (Anastassopoulou *et al.*, 2009; Berro *et al.*, 2009; Tilton *et al.*, 2010; Yoshimura *et al.*, 2009, 2010a). As shown in the present study, distinct Env sequences from each quasispecies might be selected by the different anti-HIV drugs (e.g. length of the V1/2 and/or V4 regions, V3 region depletion and the number of PNGs). Moreover, many of the novel anti-retroviral drugs in pre-clinical trials are viral entry inhibitors (e.g. PRO140, ibalizumab, BMS-663068 and PF-232798; Jacobson *et al.*, 2010; McNicholas *et al.*, 2010; Nettles *et al.*, 2011; Stupple *et al.*, 2011; Toma *et al.*, 2011). Therefore, it is necessary to examine whether such entry inhibitors are effective when used alongside conventional drugs.

In conclusion, we studied the genetic bottleneck in bulk primary HIV-1 isolates from untreated patients and drugs targeting the Env (and other) regions. The results showed, for the first time, the presence of drug-selected Env sequences in these isolates. Although our observations were based on a limited number of HIV-1 isolates and need to be confirmed by independent studies, we believe that they provide a new paradigm for HIV-1 evolution in the new combination ARV therapy era.

METHODS

Patients and isolates. Primary HIV-1 isolates were isolated from four drug-naïve patients in our laboratory (KP-1–4) and passaged in phytohaemagglutinin-activated PBMCs. Infected PBMCs were then co-cultured for 5 days with PM1/CCR5 cells (a kind gift from Dr Y. Maeda; Maeda *et al.*, 2008; Yusa *et al.*, 2005) and the culture supernatants were stored at −150 °C (Hatada *et al.*, 2010; Shibata *et al.*, 2007; Yoshimura *et al.*, 2006, 2010b).

After isolation of the primary viruses, we checked the sensitivity of each primary isolate to MVC. The KP-1 isolate was relatively MVC-resistant compared with KP-2 and KP-3 (54 vs 5.9 and 8.7 nM, respectively). KP-1 became MVC sensitive after eight passages in PM1/CCR5 cells [IC_{50}, 3.4 nM; Geno2pheno value (see below), 41.2 %], whilst under the pressure of MVC, KP-1 became highly resistant to MVC after eight passages (IC_{50}, >1000 nM; Geno2pheno value, 1.7 %). These results indicated that the bulk KP-1 isolate used in this study harboured primarily R5 viruses with X4- or dual-tropic viruses as a minor population.

Cells, culture conditions and reagents. PM1/CCR5 cells were maintained in RPMI 1640 (Sigma) supplemented with 10 % heat-inactivated FCS (HyClone Laboratories), 50 U penicillin ml^{-1}, 50 μg streptomycin ml^{-1} and 0.1 mg G418 (Nacalai Tesque) ml^{-1}. MVC, RAL and SQV were kindly provided by Pfizer, Merck & Co. and Roche Products, respectively. 3TC was purchased from Wako Pure Chemical Industries.

The laboratory-adapted HIV-1 strain 89.6, which was obtained through the NIH AIDS Research and Reference Reagent Program, was propagated in phytohaemagglutinin-activated PBMCs. The viral-competent library pJR-FL-V3Lib, which contains 176 bp V3–loop DNA fragments with 0–10 random combinations of amino acid substitutions, was introduced into pJR-FL, as described previously (Yusa *et al.*, 2005).

***In vitro* selection of HIV-1 variants using anti-HIV drugs.** The four primary HIV isolates (KP-1–4), strain 89.6 and JR-FL-V3Lib were treated with various concentrations of RAL and used to infect PM1/CCR5 cells to induce the production of RAL-selected HIV-1 variants, as described previously, with minor modifications (Hatada *et al.*, 2010; Shibata *et al.*, 2007; Yoshimura *et al.*, 2006, 2010b). Briefly, PM1/CCR5 cells (4×10^4 cells) were exposed to 500 $TCID_{50}$ HIV-1 isolates and cultured in the presence of RAL. Virus replication in PM1/CCR5 cells was monitored by observing the cytopathic effects. The culture supernatant was harvested on day 7 and used to infect fresh PM1/CCR5 cells for the next round of culture in the presence of increasing concentrations of RAL. When the virus began to propagate in the presence of the drug, the compound concentration was increased further. Proviral DNA was extracted from lysates of infected cells at different passages using a QIAamp DNA Blood Mini kit (Qiagen). The proviral DNAs obtained were then subjected to nucleotide sequencing. *In vitro* selection of the KP-1 isolate using SQV, 3TC and MVC was also performed using the procedure described above.

Amplification of proviral DNA and nucleotide sequencing. Proviral DNA was subjected to PCR amplification using PrimeSTAR GXL DNA polymerase and Ex-*Taq* polymerase (Takara), as described previously (Hatada *et al.*, 2010; Shibata *et al.*, 2007; Yoshimura *et al.*, 2006, 2010b). The primers used were 1B and H for the gp120 region (Hatada *et al.*, 2010; Shibata *et al.*, 2007; Yoshimura *et al.*, 2006, 2010b), IN 1F (5′-CAGACTCACAATATGCATTAGG-3′) and IN 1R (5′-CCTGTATGCAGACCCCAATATG-3′) for the *IN* region, and IN 1F and H for the *IN*–gp120 region. The first-round PCR products were used directly in a second round of PCR using primers 2B and F (Hatada *et al.*, 2010; Shibata *et al.*, 2007; Yoshimura *et al.*, 2006, 2010b) for gp120, IN 2F (5′-CTGGCATGGGTACCAGCACACAA-3′) and IN 2R (3′-CCTAGTGGGATGTGTACTTCTGAACTTA-3′) for *IN*, and IN 2F and F for *IN*–gp120. The PCR conditions used were as described above. The second-round PCR products were purified and cloned into a pGEM-T Easy Vector (Promega) or pCR-XL-TOPO Vector (Invitrogen), and the *env* and *IN* regions in both the passaged and selected viruses were sequenced using an Applied Biosystems 3500xL Genetic Analyzer and a BigDye Terminator v3.1 Cycle Sequencing kit (Applied Biosystems). Phylogenetic reconstructions were generated using the neighbour-joining method embedded in the MEGA software (http://www.megasoftware.net) (Tamura *et al.*, 2007). Overall, mean distances for viral diversity were also calculated using MEGA software. The number and location of putative PNGs were estimated using *N*-GlycoSite (http://www.hiv.lanl.gov/content/sequence/GLYCOSITE/glycosite.html) from the Los Alamos National Laboratory database.

Susceptibility assay. The sensitivity of the passaged viruses to various drugs was determined as described previously with minor modifications (Hatada *et al.*, 2010; Shibata *et al.*, 2007; Yoshimura *et al.*, 2006, 2010b). Briefly, PM1/CCR5 cells (2×10^3 cells per well) in 96-well round-bottomed plates were exposed to 100 $TCID_{50}$ of the viruses in the presence of various concentrations of drugs and incubated at 37 °C for 7 days. The IC_{50} values were then determined using a Cell Counting Kit-8 assay (Dojindo Laboratories). All assays were performed in duplicate or triplicate.

Predicting co-receptor usage by the V3 sequence. HIV-1 tropism was inferred using Geno2pheno [coreceptor] program, with a false rate positive (FPR) value of 5.0 %, which is freely available (http://coreceptor.bioinf.mpi-inf.mpg.de/index.php). This genotyping tool more accurately predicts virological responses to the CCR5 antagonist MVC in ARV-naïve patients than a reference phenotypic tropism test (Sing *et al.*, 2007).

Statistical analyses. Pairwise comparisons of the different parameters between variants in the two groups was calculated using the homoscedastic *t*-test. A P value of <0.05 was considered statistically significant.

ACKNOWLEDGEMENTS

We are grateful to Dr Yosuke Maeda for providing the PM1/CCR5 cells. We also thank Syoko Yamashita, Yoko Kawanami, Noriko Shirai and Akiko Shibata for technical assistance. This study was supported in part by the Ministry of Education, Culture, Sports, Science and Technology, Japan, by a Grant-in-Aid for Young Scientists (B-22790163); grants from the Ministry of Health, Labour and Welfare; the Program of Founding Research Centers for Emerging and Re-emerging Infectious Diseases; and the Global COE program Global Education and Research Center Aiming at the Control of AIDS.

REFERENCES

Anastassopoulou, C. G., Ketas, T. J., Klasse, P. J. & Moore, J. P. (2009). Resistance to CCR5 inhibitors caused by sequence changes in the fusion peptide of HIV-1 gp41. *Proc Natl Acad Sci U S A* **106**, 5318–5323.

Berro, R., Sanders, R. W., Lu, M., Klasse, P. J. & Moore, J. P. (2009). Two HIV-1 variants resistant to small molecule CCR5 inhibitors differ in how they use CCR5 for entry. *PLoS Pathog* **5**, e1000548.

Charpentier, C., Nora, T., Tenaillon, O., Clavel, F. & Hance, A. J. (2006). Extensive recombination among human immunodeficiency virus type 1 quasispecies makes an important contribution to viral diversity in individual patients. *J Virol* **80**, 2472–2482.

Delwart, E. L., Pan, H., Neumann, A. & Markowitz, M. (1998). Rapid, transient changes at the *env* locus of plasma human immunodeficiency virus type 1 populations during the emergence of protease inhibitor resistance. *J Virol* **72**, 2416–2421.

Eigen, M. (1993). The origin of genetic information: viruses as models. *Gene* **135**, 37–47.

Gulick, R. M., Lalezari, J., Goodrich, J., Clumeck, N., DeJesus, E., Horban, A., Nadler, J., Clotet, B., Karlsson, A. & other authors (2008). Maraviroc for previously treated patients with R5 HIV-1 infection. *N Engl J Med* **359**, 1429–1441.

Hatada, M., Yoshimura, K., Harada, S., Kawanami, Y., Shibata, J. & Matsushita, S. (2010). Human immunodeficiency virus type 1 evasion of a neutralizing anti-V3 antibody involves acquisition of a potential glycosylation site in V2. *J Gen Virol* **91**, 1335–1345.

Hombrouck, A., Voet, A., Van Remoortel, B., Desadeleer, C., De Maeyer, M., Debyser, Z. & Witvrouw, M. (2008). Mutations in human immunodeficiency virus type 1 integrase confer resistance to the naphthyridine L-870,810 and cross-resistance to the clinical trial drug GS-9137. *Antimicrob Agents Chemother* **52**, 2069–2078.

Ibáñez, A., Clotet, B. & Martínez, M. A. (2000). Human immunodeficiency virus type 1 population bottleneck during indinavir therapy causes a genetic drift in the env quasispecies. *J Gen Virol* **81**, 85–95.

Jacobson, J. M., Thompson, M. A., Lalezari, J. P., Saag, M. S., Zingman, B. S., D'Ambrosio, P., Stambler, N., Rotshteyn, Y., Marozsan, A. J. & other authors (2010). Anti-HIV-1 activity of weekly or biweekly treatment with subcutaneous PRO 140, a CCR5 monoclonal antibody. *J Infect Dis* **201**, 1481–1487.

Kitrinos, K. M., Nelson, J. A., Resch, W. & Swanstrom, R. (2005). Effect of a protease inhibitor-induced genetic bottleneck on human immunodeficiency virus type 1 *env* gene populations. *J Virol* **79**, 10627–10637.

Kobayashi, M., Nakahara, K., Seki, T., Miki, S., Kawauchi, S., Suyama, A., Wakasa-Morimoto, C., Kodama, M., Endoh, T. & Oosugi, E. (2008). Selection of diverse and clinically relevant integrase inhibitor-resistant human immunodeficiency virus type 1 mutants. *Antiviral Res* **80**, 213–222.

Maeda, Y., Yusa, K. & Harada, S. (2008). Altered sensitivity of an R5X4 HIV-1 strain 89.6 to coreceptor inhibitors by a single amino acid substitution in the V3 region of gp120. *Antiviral Res* **77**, 128–135.

McNicholas, P., Wei, Y., Whitcomb, J., Greaves, W., Black, T. A., Tremblay, C. L. & Strizki, J. M. (2010). Characterization of emergent HIV resistance in treatment-naive subjects enrolled in a vicriviroc phase 2 trial. *J Infect Dis* **201**, 1470–1480.

Nájera, R., Delgado, E., Pérez-Alvarez, L. & Thomson, M. M. (2002). Genetic recombination and its role in the development of the HIV-1 pandemic. *AIDS* **16** (Suppl. 4), S3–S16.

Nettles, R., Schurmann, D., Zhu, L., Stonier, M., Huang, S. P., Chien, C., Krystal, M., Wind-Rotolo, M., Bertz, R. & Grasela, D. (2011). Pharmacodynamics, safety, and pharmacokinetics of BMS-663068: a potentially first-in-class oral HIV attachment inhibitor. In *18th Conference on Retroviruses and Opportunistic Infections*, abstract 49. Boston, MA.

Nijhuis, M., Boucher, C. A., Schipper, P., Leitner, T., Schuurman, R. & Albert, J. (1998). Stochastic processes strongly influence HIV-1 evolution during suboptimal protease-inhibitor therapy. *Proc Natl Acad Sci U S A* **95**, 14441–14446.

Nora, T., Charpentier, C., Tenaillon, O., Hoede, C., Clavel, F. & Hance, A. J. (2007). Contribution of recombination to the evolution of human immunodeficiency viruses expressing resistance to antiretroviral treatment. *J Virol* **81**, 7620–7628.

Rhee, S.-Y., Liu, T. F., Kiuchi, M., Zioni, R., Gifford, R. J., Holmes, S. P. & Shafer, R. W. (2008). Natural variation of HIV-1 group M integrase: implications for a new class of antiretroviral inhibitors. *Retrovirology* **5**, 74.

Sheehy, N., Desselberger, U., Whitwell, H. & Ball, J. K. (1996). Concurrent evolution of regions of the envelope and polymerase genes of human immunodeficiency virus type 1 observed during zidovudine (AZT) therapy. *J Gen Virol* **77**, 1071–1081.

Shibata, J., Yoshimura, K., Honda, A., Koito, A., Murakami, T. & Matsushita, S. (2007). Impact of V2 mutations on escape from a potent neutralizing anti-V3 monoclonal antibody during in vitro selection of a primary human immunodeficiency virus type 1 isolate. *J Virol* **81**, 3757–3768.

Sing, T., Low, A. J., Beerenwinkel, N., Sander, O., Cheung, P. K., Domingues, F. S., Büch, J., Däumer, M., Kaiser, R. & other authors (2007). Predicting HIV coreceptor usage on the basis of genetic and clinical covariates. *Antivir Ther* **12**, 1097–1106.

Steigbigel, R. T., Cooper, D. A., Kumar, P. N., Eron, J. E., Schechter, M., Markowitz, M., Loutfy, M. R., Lennox, J. L., Gatell, J. M. & other authors (2008). Raltegravir with optimized background therapy for resistant HIV-1 infection. *N Engl J Med* **359**, 339–354.

Stupple, P. A., Batchelor, D. V., Corless, M., Dorr, P. K., Ellis, D., Fenwick, D. R., Galan, S. R., Jones, R. M., Mason, H. J. & other authors (2011). An imidazopiperidine series of CCR5 antagonists for the treatment of HIV: the discovery of N-(1S)-1-(3-fluorophenyl)-3-[(3-endo)-3-(5-isobutyryl-2-methyl-4,5,6,7-tetrahydro-1H-imidazo[4,5-c]pyridin-1-yl)-8-azabicyclo[3.2.1]oct-8-yl]propylacetamide (PF-232798). *J Med Chem* **54**, 67–77.

Tamura, K., Dudley, J., Nei, M. & Kumar, S. (2007). MEGA4: Molecular Evolutionary Genetics Analysis (MEGA) software version 4.0. *Mol Biol Evol* **24**, 1596–1599.

Tilton, J. C., Wilen, C. B., Didigu, C. A., Sinha, R., Harrison, J. E., Agrawal-Gamse, C., Henning, E. A., Bushman, F. D., Martin, J. N. & other authors (2010). A maraviroc-resistant HIV-1 with narrow cross-resistance to other CCR5 antagonists depends on both N-terminal and extracellular loop domains of drug-bound CCR5. *J Virol* **84**, 10863–10876.

Toma, J., Weinheimer, S. P., Stawiski, E., Whitcomb, J. M., Lewis, S. T., Petropoulos, C. J. & Huang, W. (2011). Loss of asparagine-linked glycosylation sites in variable region 5 of human immunodeficiency virus type 1 envelope is associated with resistance to CD4 antibody ibalizumab. *J Virol* **85**, 3872–3880.

Vignuzzi, M., Stone, J. K., Arnold, J. J., Cameron, C. E. & Andino, R. (2006). Quasispecies diversity determines pathogenesis through cooperative interactions in a viral population. *Nature* **439**, 344–348.

Yoshimura, K., Shibata, J., Kimura, T., Honda, A., Maeda, Y., Koito, A., Murakami, T., Mitsuya, H. & Matsushita, S. (2006). Resistance profile of a neutralizing anti-HIV monoclonal antibody, KD-247, that shows favourable synergism with anti-CCR5 inhibitors. *AIDS* **20**, 2065–2073.

Yoshimura, K., Harada, S., Hatada, M. & Matsushita, S. (2009). Mutations in V4 and C4 regions of the HIV-1 CRF08-BC envelope induced by the in vitro selection of Maraviroc Confer cross-resistance to other CCR5 inhibitors. In *16th Conference on Retroviruses and Opportunistic Infections*, p. 640. Montreal, Canada.

Yoshimura, K., Harada, S. & Matsushita, S. (2010a). Two step escape pathway of the HIV-1 subtype C primary isolate induced by the in vitro selection of Maraviroc. In *17th Conference on Retroviruses and Opportunistic Infections*, abstract 535. San Francisco, CA.

Yoshimura, K., Harada, S., Shibata, J., Hatada, M., Yamada, Y., Ochiai, C., Tamamura, H. & Matsushita, S. (2010b). Enhanced exposure of human immunodeficiency virus type 1 primary isolate neutralization epitopes through binding of CD4 mimetic compounds. *J Virol* **84**, 7558–7568.

Yusa, K., Maeda, Y., Fujioka, A., Monde, K. & Harada, S. (2005). Isolation of TAK-779-resistant HIV-1 from an R5 HIV-1 GP120 V3 loop library. *J Biol Chem* **280**, 30083–30090.

Zhang, Y. M., Dawson, S. C., Landsman, D., Lane, H. C. & Salzman, N. P. (1994). Persistence of four related human immunodeficiency virus subtypes during the course of zidovudine therapy: relationship between virion RNA and proviral DNA. *J Virol* **68**, 425–432.

APOBEC3G Oligomerization Is Associated with the Inhibition of Both *Alu* and LINE-1 Retrotransposition

Takayoshi Koyama[1☯], Juan Fernando Arias[1☯], Yukie Iwabu[1], Masaru Yokoyama[2], Hideaki Fujita[3], Hironori Sato[2], Kenzo Tokunaga[1*]

1 Department of Pathology, National Institute of Infectious Diseases, Tokyo, Japan, 2 Pathogen Genomics Center, National Institute of Infectious Diseases, Tokyo, Japan, 3 Faculty of Pharmaceutical Sciences, Nagasaki International University, Nagasaki, Japan

Abstract

Alu and LINE-1 (L1), which constitute ~11% and ~17% of the human genome, respectively, are transposable non-LTR retroelements. They transpose not only in germ cells but also in somatic cells, occasionally causing cancer. We have previously demonstrated that antiretroviral restriction factors, human APOBEC3 (hA3) proteins (A–H), differentially inhibit L1 retrotransposition. In this present study, we found that hA3 members also restrict *Alu* retrotransposition at differential levels that correlate with those observed previously for L1 inhibition. Through deletion analyses based on the best-characterized hA3 member human APOBEC3G (hA3G), its N-terminal 30 amino acids were required for its inhibitory activity against *Alu* retrotransposition. The inhibitory effect of hA3G on *Alu* retrotransposition was associated with its oligomerization that was affected by the deletion of its N-terminal 30 amino acids. Through structural modeling, the amino acids 24 to 28 of hA3G were predicted to be located at the interface of the dimer. The mutation of these residues resulted in abrogated hA3G oligomerization, and consistently abolished the inhibitory activity of hA3G against *Alu* retrotransposition. Importantly, the anti-L1 activity of hA3G was also associated with hA3G oligomerization. These results suggest that the inhibitory activities of hA3G against *Alu* and L1 retrotransposition might involve a common mechanism.

Citation: Koyama T, Arias JF, Iwabu Y, Yokoyama M, Fujita H, et al. (2013) APOBEC3G Oligomerization Is Associated with the Inhibition of Both *Alu* and LINE-1 Retrotransposition. PLoS ONE 8(12): e84228. doi:10.1371/journal.pone.0084228

Editor: Chen Liang, Lady Davis Institute for Medical Research, Canada

Received October 23, 2013; **Accepted** November 20, 2013; **Published** December 19, 2013

Funding: This work was supported by grants from the Ministry of Health, Labor and Welfare of Japan (Research on HIV/AIDS project no.H24-005, H24-008 and H25-010), and from the Ministry of Education, Science, Technology, Sports and Culture of Japan (22590428). The funders had no role in study design, data collection and analysis, decision to publish, or preparation of the manuscript.

Competing interests: The authors have declared that no competing interests exist.

* Email: tokunaga@nih.go.jp

☯ These authors contributed equally to this work.

Introduction

Retrotransposons compose ~42% of the human genome, and these elements are classified into the non-LTR and LTR classes. Non-LTR retrotransposons are subdivided into long interspersed elements (LINEs) and short interspersed elements (SINEs), representatives of which are LINE-1 (L1) and *Alu*, which comprise ~17% and ~11% of the human genome, respectively [1]. L1 elements harbor two ORFs: ORF1, which encodes an RNA-binding protein, and ORF2, which encodes an endonuclease-like and reverse transcriptase-like protein. After translation, these proteins bind to the L1 RNA to form a ribonucleoprotein particle that is imported into the nucleus to be integrated into the genome through target-primed reverse transcription [2-4]. Unlike L1, *Alu* elements do not encode a reverse transcriptase or an endonuclease; rather, the transcribed *Alu* RNAs hijack the L1-encoded enzymes to move to new locations in the genome through mechanisms that are as yet unclear [5]. Importantly, retrotransposition by L1 and *Alu* occurs not only in germ cells, causing several genetic diseases [6-13], but also in somatic cells, such as brain tissues [14,15], and malignant tissues and cells such as B-cell lymphoma cells [16], breast carcinoma tissue [17], colon carcinoma tissue [18], and hepatocellular carcinoma tissue [19]. These facts indicate that an intrinsic protection system should function properly to suppress these types of retrotransposition in normal somatic cells.

Human APOBEC3G (hA3G) is one of the seven members of the APOBEC3 (hA3) family of cytidine deaminases (hA3A to hA3H). hA3G is known to be an intrinsic retroviral restriction factor that inhibits Vif-defective human immunodeficiency virus type 1 (HIV-1) infection by being incorporated into viral particles and mediating extensive deamination of the nascent minus-strand viral DNA during reverse transcription, which results in G-to-A hypermutation [20-23]. This antiretroviral restriction extends to not only exogenous retroviruses, such as

simian immunodeficiency virus [24-27], primate foamy virus [28,29], human T-cell leukemia virus type I [30], murine leukemia virus [21,26,31], mouse mammary tumor virus [32], and equine infectious anemia virus [22] , but also endogenous retroelements, such as the MusD and intracisternal A-particle LTR murine retrotransposons and, as described below, human *Alu* and L1 retrotransposons ([33-40]; see also review in ref[41].). hA3G also restricts infection by hepatitis B virus, which replicates its DNA genome by reverse transcription of an RNA intermediate [42,43]. Whereas pre-primate mammals encode one, two to three A3 proteins [44], primates have acquired seven different A3 genes through 33 million years of evolution [45]. Such expansion of the hA3 genes correlates with an abrupt reduction in retrotransposition activity in primates, suggesting that these proteins have evolved to protect hosts from the genomic instability caused by retroelements [46].

We previously reported that hA3 family proteins have differential levels of anti-L1 activity that do not correlate with either antiretroviral activity or subcellular localization patterns [37]. Although several groups that performed similar studies showed that hA3G has little or no anti-L1 activity [47-50], we and others have found that the hA3G is indeed able, albeit less potently than hA3A or hA3B, to restrict L1 retrotransposition [37-40]. Such discrepancies might be attributed to the cell-type-dependent expression levels of hA3G, as we previously demonstrated [37]. We also found that hA3G inhibits L1 retrotransposition independently of its deaminase activity, which is primarily required for its antiretroviral function, and hA3G likely prevents L1 DNA synthesis *per se* [37]. With regard to the inhibition of *Alu* by hA3 family members, several groups have reported that hA3A, hA3B [49], hA3G [34-36], hA3DE, and hA3H [51] inhibit *Alu* retrotransposition. In this study, we found that all hA3 family members, from hA3A to hA3H, are able to inhibit *Alu* retrotransposition. The inhibitory effect of hA3G on *Alu* retrotransposon was associated with the N-terminal 30 amino acid residues and with hA3G's oligomerization activity, but not with its deaminase activity. Structural modeling showed that amino acid positions 24–28 are responsible for the oligomerization of hA3G. This result was verified by immunoprecipitation using an hA3G mutant with amino acid substitutions at these positions. Consistent with this result, we found that amino acid positions 24–28 of hA3G are critical for its inhibitory activity against *Alu* retrotransposon. Importantly, these amino acids were also shown to be important for L1 inhibition, suggesting that both *Alu* and L1 retrotransposition might be restricted by similar mechanisms involving hA3G, which require the oligomerization of this restriction factor.

Materials and Methods

DNA constructs

The hemagglutinin (HA)-tagged hA3 expression plasmids (phA3A-HA, phA3B-HA, phA3C-HA, phA3DE-HA, phA3F-HA, phA3G-HA, and phA3H-HA), the GFP expression plasmid pCA-EGFP, the empty expression vector pCAGGS-HA, the L1 indicator construct pCEP4/L1mneoI/ColE1 (kindly provided by N. Gilbert), the L1 ORF2 expression plasmid pBudORF2opt (kindly provided by A.M. Roy-Engel), the *Alu* indicator construct pYa5neotet (kindly provided by T. Heidmann), Vif-deficient HIV-1 proviral indicator construct pNLLuc-F(-)E(-), and VSV-G expression plasmid pHIT/G have previously been described elsewhere [5,37,52-55] (note that the hA3h expression plasmid encodes the haplotype I). The myc-tagged version of the wild-type hA3G expression plasmid, phA3G-myc, was also created. A series of N-terminal deletion mutants of hA3G (phA3G-NΔ30-HA, -NΔ60-HA, -NΔ90-HA, -NΔ120-HA, and -NΔ150-HA) were created by inserting serially deleted PCR fragments of hA3G into the mammalian expression plasmid pCAGGS with a C-terminal HA-tag. The deaminase-deficient mutant (phA3G-E259Q-HA), the oligomerization-deficient mutant (phA3G-C97/100A-HA), and the N-terminal mutants (phA3G-5G(24–28)-HA, phA3G-4G(124–127)-HA, phA3G-R24G-HA, and phA3G-Y125G-HA) of hA3G were created using phA3G-HA as a template with a QuikChange site-directed mutagenesis kit (Stratagene).

Cell maintenance, transfections, and protein analyses

HeLa and 293T cells were maintained under standard conditions. 293T cells were transfected with HA-tagged hA3 wild-type and mutant plasmids using the FuGENE 6 transfection reagent (Roche Applied Science) according to the manufacturer's instructions. Cell extracts from transfected cells were subjected to gel electrophoresis and then transferred to a nitrocellulose membrane. The membranes were probed with an anti-HA mouse monoclonal antibody (Sigma). The antibody-bound proteins were visualized to confirm hA3 protein expression by chemiluminescence using an ECL Western blotting detection system (GE Healthcare) and an LAS-3000 imaging system (FujiFilm).

Immunofluorescence microscopy

HeLa cells were plated on 13-mm glass coverslips and transfected with 0.5 μg of hA3 expressing plasmids by using FUGENE6. The transfected cells were fixed with 4% paraformaldehyde at room temperature for 30 min, permeabilized with 0.05% saponin for 10 min, and immunostained with an anti-HA monoclonal antibody (5 μg/ml). The secondary goat anti-mouse antibody that was conjugated with Cy3 was used at 5 μg/ml. All immunofluorescence images were observed on a Leica DMRB microscope (Wetzlar, Germany) equipped with a 63×1.32 NA oil immersion lens (PL APO), acquired through a cooled CCD camera, MicroMAX (Princeton Instruments, Trenton, NJ), and digitally processed using IPlab Software (Scanalytics, Fairfax, VA). All images were assembled using Adobe Photoshop (Adobe Systems, Mountain View, CA).

L1 and Alu retrotransposition assay

L1 and *Alu* retrotransposition assays were performed by co-transfecting 2 x 10^5 HeLa cells with 0.1 μg of the respective hA3 expression plasmid (or a mock expression vector, pCAGGS-HA, as a positive control) together with either 0.3 μg of the neomycin-resistance (neo^r)-based L1 expression vector pCEP4/L1mneoI/ColE1 and 0.1 μg of an empty vector (for the